



HAL
open science

Direct Access to Palladium(II) Complexes Based on Anionic C , C , C -Phosponium Ylide Core Pincer Ligand

Rachid Taakili, Cécile Barthes, Christine Lepetit, Carine Duhayon, Dmitry A. Valyaev, Yves Canac

► **To cite this version:**

Rachid Taakili, Cécile Barthes, Christine Lepetit, Carine Duhayon, Dmitry A. Valyaev, et al.. Direct Access to Palladium(II) Complexes Based on Anionic C , C , C -Phosponium Ylide Core Pincer Ligand. *Inorganic Chemistry*, 2021, 60 (16), pp.12116-12128. 10.1021/acs.inorgchem.1c01316 . hal-03357270

HAL Id: hal-03357270

<https://hal.science/hal-03357270>

Submitted on 28 Sep 2021

HAL is a multi-disciplinary open access archive for the deposit and dissemination of scientific research documents, whether they are published or not. The documents may come from teaching and research institutions in France or abroad, or from public or private research centers.

L'archive ouverte pluridisciplinaire **HAL**, est destinée au dépôt et à la diffusion de documents scientifiques de niveau recherche, publiés ou non, émanant des établissements d'enseignement et de recherche français ou étrangers, des laboratoires publics ou privés.

Direct Access to Palladium(II) Complexes Based on Anionic C,C,C-Phosphonium Ylide Core Pincer Ligand

Rachid Taakili, Cécile Barthes, Christine Lepetit, Carine Duhayon, Dmitry A. Valyaev* and Yves Canac*

LCC-CNRS, Université de Toulouse, CNRS, 205 route de Narbonne, 31077 Toulouse Cedex 4, France

ABSTRACT: The reaction of readily available imidazolium-phosphonium salt [MesIm(CH₂)₃PPh₃](OTf)₂ with PdCl₂ in the presence of an excess of Cs₂CO₃ afforded selectively in one step the cationic Pd(II) complex [(C,C,C)Pd(NCMe)](OTf) exhibiting LX₂-type NHC-ylide-aryl C,C,C-pincer ligand *via* formal triple C–H bond activation. The replacement of labile MeCN in the latter by CN*t*Bu and CO fragments allowed to estimate the overall electronic properties of this phosphonium ylide core pincer scaffold incorporating three different carbon-based donor ends by IR spectroscopy, cyclic voltammetry and molecular orbital analysis revealing its significantly higher electron-rich character compared to structurally close NHC core pincer system with two phosphonium ylide extremities. The pincer complex [(C,C,C)Pd(CO)](OTf) represents a rare example of Pd(II) carbonyl species stable at room temperature and characterized by X-ray diffraction analysis. The treatment of isostructural cationic complexes [(C,C,C)Pd(NCMe)](OTf) and [(C,C,C)Pd(CO)](OTf) with (allyl)MgBr and *n*BuLi led to the formation of zwitterionic phosphonium organopalladates [(C,C,C)PdBr] and [(C,C,C)Pd(COBU)], respectively.

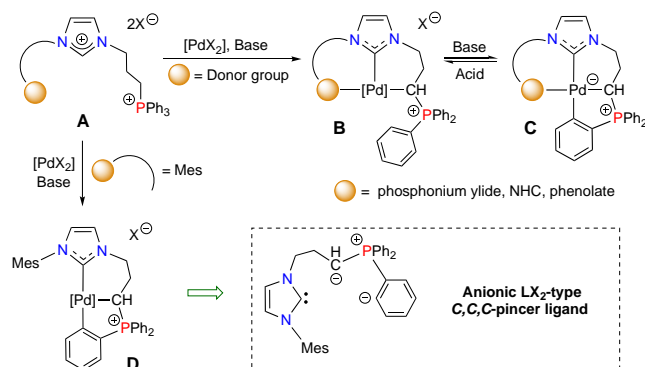
INTRODUCTION

The preparation of the first pincer complex by Moulton and Shaw in the late 70s played a decisive role in the rapid development of modern organometallic chemistry and homogeneous catalysis.¹ Following this pioneering report, a wide variety of pincer architectures differing in the nature of the backbone, the coordinating extremities, and the metallacycle ring size were designed.² Thanks to the unique meridional geometry of these robust and constrained metallic systems, unusual bonding modes and peculiar reactivities were observed resulting in a large number of applications, especially in the field of homogeneous catalysis.³ In line with our continued efforts to design ligands that push the limits of the electronic parameter scale, whether extremely electron-poor⁴ or electron-rich,⁵ we have recently focused on the preparation of pincer ligands exhibiting only carbon-based donor extremities. Although this category of ligands is of particular interest because of their strong electron-donating character, related C,C,C-pincer complexes are scarce due to the lack of general synthetic methods and thus their chemistry remain underdeveloped compared to those featuring heteroatom-based (N, O, P, S) donor moieties.² The initial development of this research area dealt with the replacement of phosphine arms in the L₂X-type [PC₂sp²P] pincer prototype by NHC moieties.⁶ The preparation of dianionic LX₂-type cyclometallated NHC⁷ and carbodiphosphorane core complexes,⁸ as well as the combination of three NHC⁹ and three aryl¹⁰ moieties in respective L₃- and X₃-type pincer complexes were considered later on. Our original contribution was based on the association of ubiquitous sp²-type NHCs¹¹ with sp³-type phosphonium ylides,¹² the latter being just like the NHCs, globally neutral in their free state behaving as strong σ-donors and effective Lewis bases in main-group¹³ and coordination chemistry.¹⁴ Chelating ligands combining these two carbon donor moieties

linked by a flexible -(CH₂)₃- bridge¹⁵ were recently prepared in the bidentate,¹⁶ pincer¹⁷ and tetradentate¹⁸ series, and their coordination behavior was studied towards various Pd(II) centers. It was also reported that NHC-phosphonium ylide pincer complexes were active in the Pd-catalyzed allylation of aldehydes.^{17b}

“On the way” to NHC core phosphonium ylide-based pincer Pd(II) complexes of type **B** from readily available *N*-phosphonio-substituted imidazolium salts **A**, original *ortho*-metalated Pd(II) complexes **C** resulting from the base-assisted C–H bond activation of one of the P⁺-phenyl rings were isolated, this process being totally reversible under acidic conditions (Scheme 1, *top*).¹⁷ Taking advantage of this reactivity, one may wonder if the replacement of one the two *N*-donor arms of the NHC core by a ‘spectator’ *N*-substituent such as a mesityl group would not allow access to complexes **D** supported by an anionic LX₂-type pincer ligand derived from a central phosphonium ylide bearing NHC and phenyl donor arms (Scheme 1, *bottom*).

Scheme 1. Preparation of C,C,C-Pincer Pd(II) Complexes featuring NHC and Phosphonium Ylide Cores from *N*-Phosphonio-Substituted Imidazolium Salts

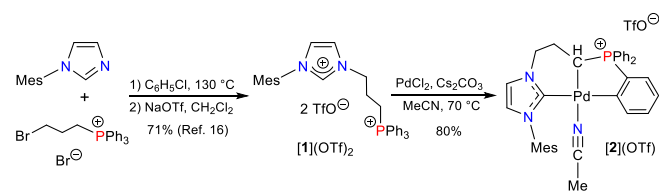


In this context, we describe herein the straightforward preparation of Pd(II) complexes bearing unprecedented type of *C,C,C*-pincer ligand, their structural investigation and original reactivity with nucleophiles. Additionally, electron-donating properties of this new ligand system have been experimentally and theoretically evaluated revealing the critical role of the phosphonium ylide core.

RESULTS AND DISCUSSION

Synthesis and Spectroscopic Characterization of Cationic Phosphonium Ylide Core Pincer Pd(II) Complexes. To test our hypothesis, 1-mesityl-3-(3-(triphenylphosphonio)propyl)imidazolium salt **[1](OTf)**₂ readily prepared from 1-mesitylimidazole and (3-bromopropyl)triphenylphosphonium bromide followed by Br⁻/OTf⁻ anion exchange according to a recently reported procedure was selected as the starting material (Scheme 2).¹⁶ While no reaction between stoichiometric amounts of **[1](OTf)**₂ and PdCl₂ in the presence of 5 equiv. of Cs₂CO₃ was observed in CH₃CN at room temperature, a clean transformation occurred at 70 °C affording the Pd(II) pincer complex **[2](OTf)** isolated in 80% yield (Scheme 2). Remarkably, the formation of **[2](OTf)** involved the selective base-assisted activation of three C–H bonds¹⁹ and this complex was found to be perfectly air-stable both in the solid state and in solution. The ³¹P NMR spectrum of **[2](OTf)** displayed a single signal at δ_p 33.5 ppm (Table 1), thus shifted to low field with respect to the phosphonium precursor **[1](OTf)**₂ (δ_p 23.8 ppm). The coordination of the NHC moiety to the metal atom in **[2](OTf)** was evidenced by the disappearance of the ¹H signal of the imidazolium proton of **[1](OTf)**₂ and the observation of the characteristic N₂C carbon resonance (δ_c 176.6 ppm (d, J_{CP} = 5.5 Hz) in the ¹³C NMR spectrum strongly deshielded with respect to the N₂CH carbon atom of **[1](OTf)**₂ (δ_{CH} 136.9 ppm).¹⁶ ¹³C NMR spectroscopy also unveiled the resonances of the CH ylide at δ_{CH} 19.5 ppm (d, J_{CP} = 43.3 Hz) and of the *ortho*-metallated carbon atom at δ_c 175.2 ppm (d, J_{CP} = 33.9 Hz) in agreement with the concomitant coordination of three carbon atoms of different nature to the Pd(II) center (Scheme 2, Table 1). Interestingly, the ¹³C NMR signal of phosphonium ylide in the central position was shifted low-field by 10–15 ppm compared to similar Pd(II) pincer complexes incorporating the same moiety at the lateral position (5.7–9.9 ppm).¹⁷ The presence of coordinated CH₃CN in **[2](OTf)** was established on the basis of corresponding ¹H and ¹³C NMR signals observed in CD₂Cl₂ solution at δ_H 1.92 ppm and δ_c 1.1 ppm, respectively. Finally, the cationic character of complex **[2](OTf)** was confirmed by ESI mass spectroscopy (*m/z* 634.2 [M – OTf]⁺).

Scheme 2. Synthesis of Phosphonium Ylide Core Pincer Pd(II) complex **[2](OTf)**



In order to get some insights into the electronic properties of the novel *C,C,C*-pincer ligand, the displacement of the CH₃CN ligand in **[2](OTf)** by isocyanide and CO was next performed (Scheme 3). For this purpose, complex **[2](OTf)** was treated

with *t*BuNC in CH₂Cl₂ at –78 °C affording the targeted adduct **[3](OTf)** in 94% yield (Scheme 3, *left*). While the ¹³C NMR NMR signals of the pincer backbone remained essentially unchanged compared to precursor **[2](OTf)**, the coordination of the isocyanide was evidenced by the broad resonance at δ_c 138.4 ppm assigned to the carbon atom directly attached to the metal center accompanied with two characteristic resonances of the *t*Bu group at δ_c 58.0 and 30.1 ppm (Table 1). The IR spectrum of **[3](OTf)** in a CH₂Cl₂ solution confirmed the existence of a strong ν_{C=N} band at 2187 cm⁻¹ consistent with a Pd(II) coordinated isocyanide.^{17,20}

Scheme 3. Substitution of MeCN Ligand at the Pd(II) Center in Complex **[2](OTf)** with *t*BuNC and CO

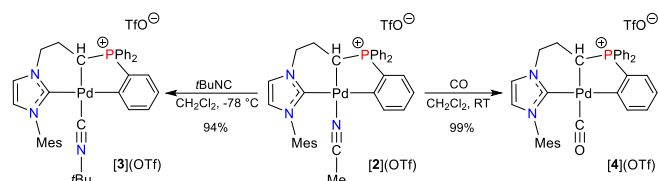


Table 1. Selected ³¹P and ¹³C NMR Chemical Shifts (ppm) in CD₂Cl₂ Solution with Signal Multiplicity and J_{CP} Coupling Constants (Hz) in Parenthesis for Pd(II) Pincer Complexes **[2](OTf), **[3](OTf)**, **[4](OTf)**, **5** and **6**.**

	[2](OTf)^a	[3](OTf)	[4](OTf)	5	6^b
δ _p	33.5 (s)	33.5 (s)	35.8 (s)	29.8 (s)	18.8 (brs)
δ _{N₂C}	176.6 (d, 5.5)	176.4 (d, 6.1)	174.0 (d, 5.1)	181.7 (d, 6.0)	183.3 (d, 6.1)
δ _{C^{Ph}}	175.2 (d, 33.9)	172.5 (d, 32.6)	169.2 (d, 31.1)	178.0 (d, 33.2)	181.3 (d, 31.3)
δ _{CH}	19.5 (d, 43.3)	22.3 (d, 40.3)	27.9 (d, 43.3)	18.7 (d, 42.3)	17.5 (d, 43.4)
δ _{C(L)^c}	–	138.4 (brs)	180.5 (d, 5.9)	–	277.1 (brs)

^a NMR data was recorded in CD₃CN. ^b NMR data was recorded in THF-D₈. ^c L corresponds to the ligand *trans* coordinated to the central phosphonium ylide fragment.

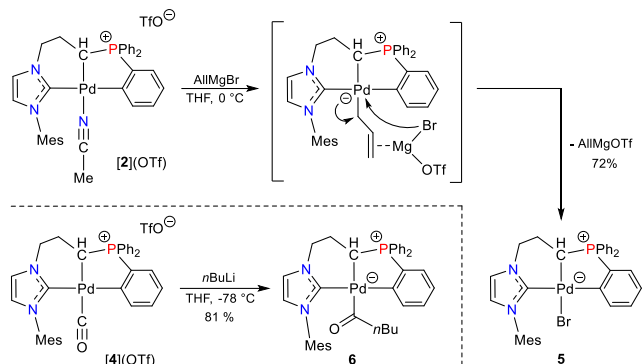
To perform the MeCN/CO ligand exchange at the metal center, CO gas was bubbled through a solution of complex **[2](OTf)** in CH₂Cl₂ at room temperature (Scheme 3, *right*). Gratifyingly, a quantitative formation of the new product **[4](OTf)** was achieved after only 15 min as revealed by ³¹P NMR monitoring with the appearance of a singlet at δ_p 35.8 ppm. The presence of the Pd–CO bond in **[4](OTf)** was unambiguously demonstrated by the low-field doublet observed at δ_c 180.5 (d, J_{CP} = 5.9 Hz) in the ¹³C NMR spectrum (Table 1) and the observation of a strong IR ν_{C=O} band at 2105 cm⁻¹ in CH₂Cl₂ solution. The analysis of ¹³C NMR spectra for complexes **[2–4](OTf)** revealed the gradual downfield shift of the phosphonium ylide resonance upon the increase of ligand π-acidity (MeCN < *t*BuNC < CO), while the signals of NHC and aryl moieties showed the opposite trend albeit in a smaller extent (Table 1). It is noteworthy, that **[4](OTf)** belongs to rare examples of Pd(II) pincer carbonyl complexes perfectly stable at room temperature even under high vacuum²¹ making possible, in particular, to record its mass spectrum (**4⁺**: *m/z* 621.1 [M–OTf]⁺) and determine the X-ray structure (*vide infra*).

“Having in hands” the efficient protocol for the synthesis of a new family of Pd(II) complexes based on pincer ligands containing phosphonium ylide moiety scarcely reported in the literature,^{17,22} we turned next our attention to the preliminary studies of the reactivity of these organometallic derivatives.

Reactions of Cationic Pd(II) Phosphonium Ylide Core Pincer Complexes [2](OTf) and [4](OTf) with Nucleophiles to Form Zwitterionic Palladate Derivatives 5-6. Taking into account the highly electron-rich character of our *C,C,C*-pincer ligand we considered that cationic phosphonium ylide core Pd(II) complexes [2-4](OTf) could serve as valuable precursors for the formation of zwitterionic metallate species containing positively charged fragments more or less distant from the metal atom.²³ In order to validate this proposal, we first tried the reaction of [2](OTf) with one equiv. of (allyl)MgBr in THF with the aim to isolate the corresponding η^1 -allyl Pd complex, as such species were reported to be the key intermediates in catalytic allylation of aldehydes with Bu₃Sn(allyl).^{17b,24} Although a clean formation of a new complex 5 with a ³¹P NMR signal at δ_p 29.8 ppm slightly shifted to high field compared to [2-4](OTf) was observed after 2 hours at RT (Scheme 4, top), no spectroscopic evidence for the presence of the allyl moiety was obtained. The signals of N₂C and *ortho*-metallated carbon atoms in 5 were found to be deshielded at δ_c 181.7 (d, J_{CP} = 6.0 Hz) and δ_c 178.0 (d, J_{CP} = 33.2 Hz) respectively, while the doublet of the CH ylide was shifted to high field at δ_c 18.7 (d, J_{CP} = 42.3 Hz) with respect to complexes [2-4](OTf) (Table 1). These NMR resonances were finally attributed to the formation of a zwitterionic Pd–Br pincer complex whose the structure was unambiguously confirmed by X-ray diffraction study. It is worth mentioning that the bromide in 5 can be readily displaced by a large excess of MeCN giving back the complex [2](OTf). In order to rationalize this unexpected reactivity, complex [2](OTf) was treated with different conventional brominating agents such as [Et₄N]Br (MeCN, 80°C, 48 h), MgBr₂ (CH₂Cl₂, 25°C, 24 h) or *N*-bromosuccinimide (CH₂Cl₂, 25°C, 2 h). While no reaction was evidenced in the two first cases, the formation of intractable mixture of products was observed in the latter case. Based on this and the results observed in the NHC-bis(ylide) series,^{17b} we propose that a highly nucleophilic η^1 -allyl-coordinated Pd pincer intermediate²⁴ initially obtained from (allyl)MgBr and [2](OTf) underwent activation by the strong Lewis acid MgBr(OTf) released in the medium to form the experimentally observed Pd–Br complex 5 (Scheme 4, top).

Another zwitterionic organopalladate was obtained during the attempt to generate a metallated ylide²⁵ by the deprotonation of the [P⁺–CH] moiety in carbonyl complex [4](OTf). Indeed, the formation of zwitterionic pincer Pd–acyl complex 6 isolated in 81% yield was observed as a result of nucleophilic addition

Scheme 4. Synthesis of Zwitterionic Phosphonium Ylide Core Pincer Pd(II) Complexes 5 and 6 from their Cationic Precursors [2](OTf) and [4](OTf), Respectively



of *n*BuLi to the CO ligand. Though such reactivity with organolithium compounds is common for group 6-8 transition metal carbonyl complexes to the best of our knowledge it is unprecedented for palladium derivatives. The ³¹P NMR spectrum of zwitterion 6 displayed a broad singlet at δ_p 18.8 ppm, significantly shifted to high field compared to previous Pd(II) *C,C,C*-pincer complexes regardless of their overall charge (Table 1). The Pd coordination of the COBu fragment was unambiguously established by the broad strongly deshielded ¹³C NMR signal at δ_c 277.1 ppm. Finally, in the IR spectrum of 6 in THF solution, the $\nu_{C=O}$ band appeared at 1607 cm⁻¹, a value substantially lower than those generally observed for Pd(II) acyl complexes (ca. 1670–1680 cm⁻¹).²⁶

The formation of zwitterionic Pd(II) complexes 5 and 6 bearing X-type bromide and acyl co-ligands, respectively and characterized by a weak charge separation reflects to some extent the strong donating character of the phosphonium ylide core pincer ligand, either exalting the nucleophilicity of the metal-bound allyl fragment, or preventing the further deprotonation of the [P⁺–CH] coordinating extremity.

X-ray Diffraction Structural Studies of Phosphonium Ylide-Core Pincer Pd(II) Complexes [2](OTf), [3](OTf), [4](OTf), and 5. Single-crystal X-ray diffraction studies allowed us to establish the solid state structures of cationic pincer Pd(II) complexes [2-4](OTf) and zwitterionic Pd(II) complex 5 (Figure 1).²⁷ The most pertinent metrical data are presented in Table 2. In all cases, the Pd(II) atom resides in a square planar environment being part of strongly distorted fused six and five-membered metallacycles, the latter incorporating the phosphonium moiety. The value of tau parameter (τ_4) close to 0 indicates a small deviation from the square planar geometry (Table 2).²⁸ While the central phosphonium ylide coordinating end is located in *trans* position relative to the neutral (L = NCMe, CN*t*Bu, CO) or anionic (X = Br) ligand (C6–Pd–L/X: 172.16(6)–172.8(2)°), the NHC and the phenyl donor moieties adopt a mutual *trans* arrangement (C1–Pd–C8: 172.82(6)–174.0(2)°). The deviation observed for the ideal linear Pd–L (L = NCMe, CN*t*Bu, CO) coordination mode in complexes [2-4](OTf) (Pd–L : 172.43(14)–175.4(5)°) might be partially caused by the steric demand of the *N*-Mes substituent. In the zwitterionic Pd–Br complex 5, the electron-withdrawing effect of bromine atom stabilizes the charge separation and consistently, the Pd–Br bond is indeed quite long (Pd–Br: 2.5083(4) Å), as compared to that occurring for instance in the neutral pincer [PCP]PdBr complex (2.495(1) Å).²⁹

Remarkably, the replacement of MeCN by more π -acceptor CN*t*Bu and CO moieties results in the counterintuitive elongation of the C6–Pd bond with concomitant shortening of both

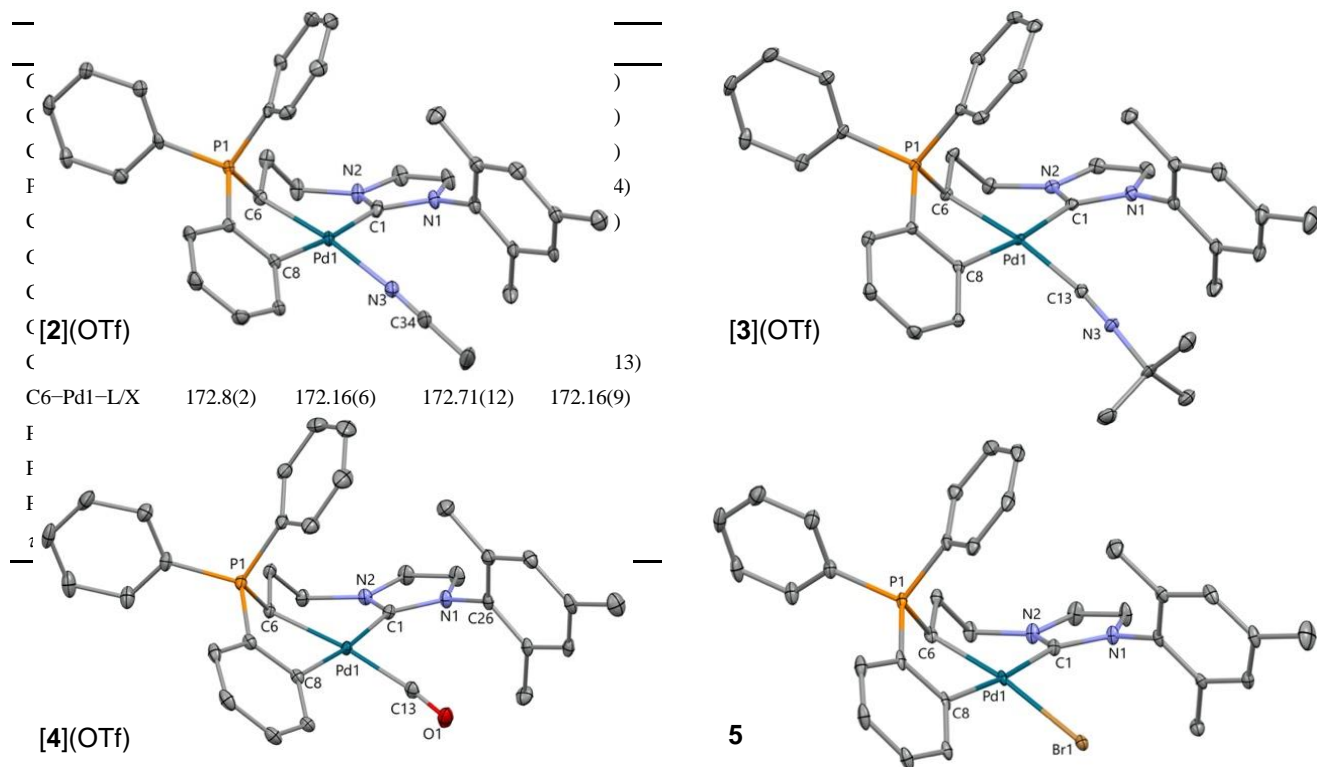


Figure 1. Perspective views of phosphonium ylide core Pd(II) complexes [2](OTf), [3](OTf), [4](OTf), and **5** with thermal ellipsoids drawn at the 30% probability level. Hydrogen atoms and TfO⁻ anions are omitted for clarity.

C1–Pd and C8–Pd bond distances. These changes in Pd–phosphonium ylide distances could be tentatively rationalized by the superior *trans* influence³⁰ of CN*t*Bu and CO fragments compared to that of MeCN,³¹ which would thus induce the lengthening of the *trans* Csp³–Pd bond of the central ylide extremity. This implies also that the donation of the NHC and the phenyl ring is sufficient to compensate the electronic deficiency at the metal caused by the introduction of an electron-accepting ligand. Although to a lesser extent, the same trend in the Pd–C bond distances was observed in the Pd–Br complex **5**. The shortening of the Pd–isonitrile bond (Pd–C13: 1.9985(16) Å) in complex [3](OTf) along with the corresponding lengthening of the C≡N bond distance (C13–N3: 1.149(2) Å) compared to those observed in previously reported NHC core, bis(phosphonium ylide) Pd–CN*t*Bu pincer complexes (Pd–C: 2.010(3)–2.013(9) Å; C–N: 1.126(10)–1.141(4) Å) suggest the stronger donor character of the ylide core pincer ligand.^{17a}

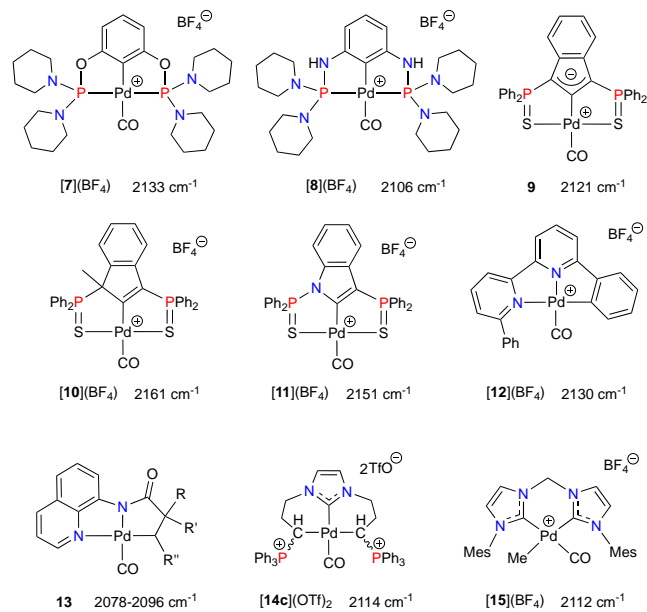
Carbonyl Pd(II) complexes stable at room temperature remain rare due to their strong ability to insert CO into a Pd–C σ-bond to form Pd acyl derivatives.³² In the pincer series (Scheme 5), only few ligands based on *P,C,P*-diphosphinoaryl ([**7–8**](BF₄)),³³ *S,C,S*-indolyl (**9**, [**10–11**](BF₄)),³⁴ *N,N,C*-diaminoaryl ([**12**](BF₄)),³⁵ *N,N,C*-8-amino(amido)(alkyl) (**13**)²¹ and *C,C,C*-NHC, bis(phosphonium ylide) ([**14c**](OTf)₂)^{17a} structures were reported to stabilize Pd–CO adducts. Structurally identified Pd(II) carbonyl pincer complexes are even rarer, since only Pd complexes of type **13** were characterized by X-diffraction analysis, thanks to the presence of the strongly σ-donating dianionic amido(alkyl) ligand.²¹

Table 2. Selected Bond Lengths (Å) and Valent Angles (°) for Pd(II) Pincer Complexes [2–4](OTf) and 5.

Table 2. Selected Bond Lengths (Å) and Valent Angles (°) for Pd(II) Pincer Complexes [2–4](OTf) and **5**.

Table 2. Selected Bond Lengths (Å) and Valent Angles (°) for Pd(II) Pincer Complexes [2–4](OTf) and **5**.

To our knowledge, a sole example of Pd–CO complex [**15**](BF₄) (Scheme 5) featuring a bulky bidentate bis(NHC) ligand and was analyzed in the solid state,³⁶ while no example bearing Scheme 5. Known Pd(II) Carbonyl Complexes Bearing Pincer-Type and Bis-NHC Ligands with Corresponding ν_{CO} Band Frequencies

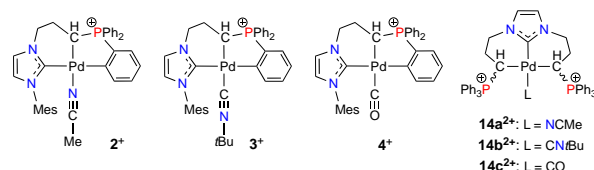


an ylide ligand was reported. In the complex [4](OTf), the C–O bond distance of 1.117(4) Å is longer than in the bis(NHC) complex [**15**](BF₄) (1.059(5) Å)³⁶ indicating stronger π-back-bonding from the Pd atom in agreement with the superior donor

ability of phosphonium ylides compared to NHCs.^{15b} Interestingly, the Pd–CO fragment in complex [4](OTf) was found to significantly deviate from the expected linear geometry (Pd1–C13–O1 172.7(3)°) accompanied with a close proximity between the C_{ipso} carbon atom of the mesityl group and the coordinating carbon atom (C13...C26: 3.055(4) Å) inferior to the sum of the Van der Waals radii (3.4 Å) suggesting the occurrence of weak attractive π(C=C)...π*C≡O interaction (*vide infra*).³⁷

IR Spectroscopy, Cyclic Voltammetry, and Theoretical Studies of Pd(II) Phosphonium Ylide-Core Pincer Complexes [2-4](OTf). The electronic properties of the ylide core pincer ligand of Pd(II) complexes [2-4](OTf) were studied by a combination of experimental methods and theoretical calculations (Table 3). The examination of experimental ν_{CO} frequency value of carbonyl complex [4](OTf) (2105 cm⁻¹) and those of related cationic Pd(II) species (Scheme 5) revealed that among L₂X-type ligands only *P,C,P*-pincer bearing highly electron-rich tri(amino)phosphine extremities in complex [8](BF₄) (ν_{CO} 2106 cm⁻¹)³³ is comparable with ylide core *C,C,C*-pincer in terms of electron-donation. It was found that among LX₂-type ligands only the family of amino(amido)alkyl pincers (Scheme 5, **13**)²¹ showed superior electronic donation than our ligand system. In contrast, the ν_{CO} value for Pd(II) complex [14c](OTf)₂ exhibiting the *C,C,C*-NHC core, bis(phosphonium ylide) pincer ligand (2114 cm⁻¹)¹⁷ was *ca.* 9 cm⁻¹ higher than for [4](OTf). Similar trend was also observed in ν_{CN} frequencies in Pd(II) isocyanide complexes [3](OTf) and [14b](OTf)₂ measured at 2187 and 2194 cm⁻¹, respectively (Table 3). These IR data unambiguously show that among the two carbon-based pincer families the ylide core ligand is more electron-donating than its NHC core analogue.

Table 3. Experimental and Calculated IR ν_{CO} and ν_{CN} Stretching Frequencies (cm⁻¹), and E_p^{ox} (V) for the Cationic Pd Complexes 2⁺, 3⁺, 4⁺ and 14a-c²⁺.^{17b}



The structures show Pd(II) complexes with a pincer ligand (NHC or ylide core) and a phosphonium ylide group. 2+ has a methyl group, 3+ has an isobutyl group, and 4+ has a carbonyl group. 14a-c2+ are bis-phosphonium ylide complexes with different ligands L: NCMe (14a), CNtBu (14b), and CO (14c).

ν _{CN} (exp) ^a	—	2187	—	14b ²⁺ : 2194
ν _{CN} (calcd) ^b	2304	2195	—	14b ²⁺ : 2203
D (calcd - exp)	—	8	—	9
ν _{CO} (exp) ^a	—	—	2105	14c ²⁺ : 2114
ν _{CO} (calcd) ^b	—	—	2073	14c ²⁺ : 2078
D (calcd - exp)	—	—	32	36
E _p ^{ox} ^c	1.6	1.8	2.1	14a ²⁺ : 1.6

^a IR frequency values measured in CH₂Cl₂ solution. ^b Calculations were performed at the PBE-D3/6-31G**/LANL2DZ*(Pd) level. ^c E_p^{ox} values (V) are given vs. SCE.

Though two LX₂-type ligand families are similar in terms of bonding mode according to the Green formalism,³⁸ the stronger donation of ylide core system may be tentatively assigned to the difference in overall ligand charge. Indeed, the ylide core ligand is anionic in nature, whereas the NHC core, bis(ylide) analogue is globally neutral.

With the aim to get further insights into the electronic structure and bonding of novel *C,C,C*-pincer ligand, the structure of cations [2-4]⁺ was calculated at the PBE-D3/6-31G**/LANL2DZ*(Pd) level. Calculated ν_{CO} and ν_{CN} frequency values in complexes [3-4]⁺ were found to be lower than for the corresponding NHC, bis(ylide) analogues [14b-c]²⁺ (Table 3) thus reproducing the experimental observations. Selected molecular orbitals (MOs) of complexes [2-4]⁺ are shown in Figure 2. Along the series (2⁺ → 3⁺ → 4⁺), the highest occupied molecular orbitals (HOMOs) and the lowest occupied molecular orbitals (LUMOs) are globally shifted to deeper energy. In all complexes, the HOMO involves a strong contribution of the d orbitals of the metal atom featuring d_{z²} character for [2-3]⁺ and d_{xz} character for 4⁺. In the latter, the HOMO shows also a significant contribution of the π orbitals of the NHC and phenyl rings. Noticeably, the phosphonium moiety and the ligand situated in *trans* position to the ylide systematically contribute for the LUMOs. While the LUMOs for [2-3]⁺ are strongly localized on the π system of the phosphonium, in case of carbonyl complex 4⁺ this orbital corresponds to the π*(CO). In complexes [2-3]⁺, the π*(CN) mixing with other delocalized π-bonds occurs at higher energy, as illustrated by the LUMO+2.

These MO feature foreshadow the analysis of experimental oxidation potentials (E_p^{ox}) determined by cyclic voltammetry (Table 3). Considering that the ylide core pincer remains the same along the series, the E_p^{ox} values are therefore expected to reflect the electronic endowment of the co-ligand (MeCN vs. *t*BuNC vs. CO) in corresponding Pd(II) complexes [2-4](OTf). All oxidations were found to be irreversible showing variation as a function of the σ-donation vs. π-accepting properties of the co-ligand ([2](OTf): 1.6 V < [3](OTf): 1.8 V < [4](OTf): 2.1 V).³⁹ In accordance with the relative energy of HOMOs (HOMO energy for 2⁺: -7.4 eV; 3⁺: -7.6 eV; 4⁺: -8.1 eV), the Pd complex [2](OTf) containing acetonitrile ligand is the more easily oxidized with a E_p^{ox} value in the same range as that of the NHC, bis(ylide) Pd(II) complex [14a](OTf)₂ (Table 3).^{17b} The similarity of the E_p^{ox} values between these two Pd-MeCN adducts, expected to be different, might be due to the large width of the irreversible oxidation waves preventing the measure of a very accurate value. By contrast to [2](OTf), complex [4](OTf) bearing CO ligand is more reluctant to oxidation as illustrated with their relative HOMO energies. These E_p^{ox} values clearly demonstrate that the redox event is Pd-centered, in perfect line with the IR frequencies and the determination of MOs.

In order to rationalize the particular stability of Pd(II) carbonyl complex [4]⁺ its electronic structure and the bonding interactions were further investigated using various QTAIM descriptors and compared with those of Pd(II) carbonyl complex [14c]²⁺ (Figure 3, Table 4). According to the classification of Bianchi *et al.*,⁴⁰ the |V_{bcp}|/G_{bcp} ratio (1.32) for the Pd–CO bonds refers in both cases to the intermediate bond regime (1 < |V_{bcp}|/G_{bcp} < 2) located between ionic and covalent bonding. Based on the Macchi's classification,⁴¹ their large electron density values (ρ_{bcp} ≥ 0.131 a.u.), their large positive Laplacian densities (Δρ_{bcp} ≥ 0.444 a.u.) and negative energy densities H_{bcp}, are in favor of a dative bond of significant covalent character (Table 4). Values of DI (≈ 1.0) and |H_{bcp}|/ρ_{bcp} (≈ 0.40) indicate a strong covalence degree of these Pd–CO bonds. Despite the apparent similarity of the nature of the Pd–CO bond in both

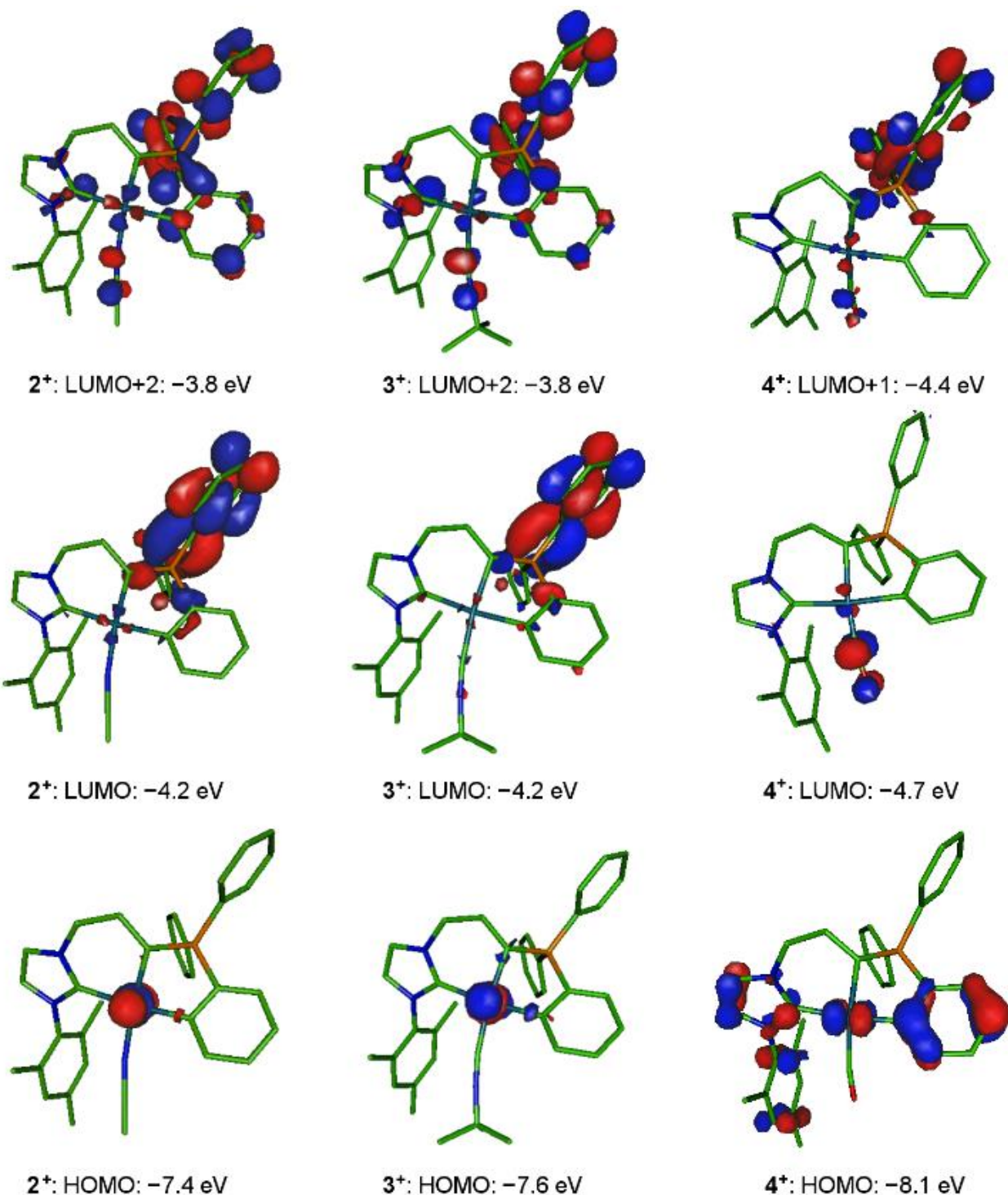


Figure 2. Selected frontier molecular orbitals (energies in eV) of Pd(II) pincer complexes 2^+ (L = NCMe, *left*), 3^+ (L = CNtBu, *middle*) and 4^+ (L = CO, *right*). PBE-D3/6-31G**/LANL2DZ*(Pd) level of calculation.

complexes, its bond strength (E_{int}) estimated using Espinosa-Molins-Lecomte approach⁴² was calculated to be larger for the ylide core pincer complex [4^+] than for the NHC core pincer complex [$14c^{2+}$] (70.4 vs. 67.7 kcal.mol⁻¹, respectively). The latter E_{int} values and the above QTAIM descriptors of the Pd–CO bonds are in the same range as those calculated for Cu(I)–CO bonds in zeolites.⁴³ As suggested by the X-ray structure of Pd complex 4^+ (*vide supra*), a weak attractive non-bonding C=C...C=O interaction³⁷ was confirmed by the presence of

the bond critical point between the corresponding C_{ipso} and carbonyl carbon atoms and its energy was estimated to be about 1.7 kcal.mol⁻¹. While such interligand bonding is more common for carbonyl-containing transition metal NHC complexes exhibiting (pseudo)octahedral, tetrahedral and trigonal bipyramidal geometry,^{37a} the examination of CCDC base revealed only two examples of square-planar Rh(I) complexes based on chelating bidentate NHC ligands, which display similar structural features as observed in the complex [4](OTf).⁴⁴ The same

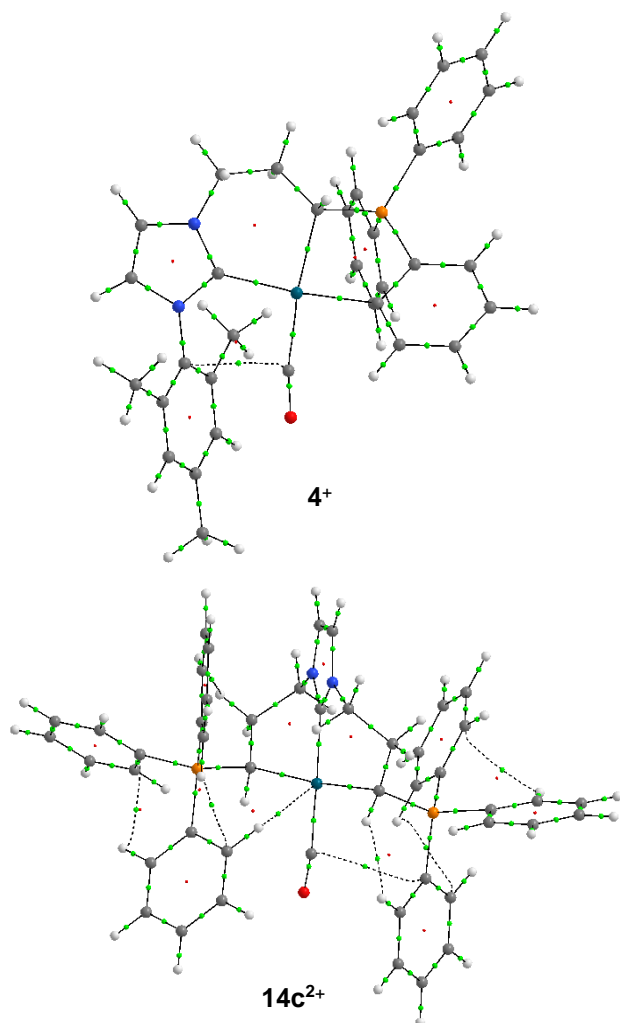


Figure 3. QTAIM molecular graphs of Pd complexes $[4^+]$ (top) and $[14c^{2+}]$ (bottom) calculated at the PBE-D3/6-31G**/LANL2DZ*(Pd) level. Bond critical points and ring critical points are shown as small green and red spheres, respectively. Element color code: C – grey, H – white, N – blue, O – red, P – orange, Pd – green-blue. Weak interactions with ≤ 0.0795 au are not visible.

Table 4. QTAIM descriptors (in a.u.) of the Bond Critical Points (BCP) related to Pd–CO bonds and C=C...C=O in Pd(II) Complexes 4^+ and $14c^{2+}$ illustrated in Figure 3. PBE-D3/6-31G**/LANL2DZ*(Pd) level of calculation.

BCP	Pd–CO (4^+)	C=C...C=O (4^+)	Pd–CO ($14c^{2+}$)	C=C...C=O ($14c^{2+}$)
ρ_{bcp}	0.1360	0.0113	0.1316	0.0803
$\Delta\rho_{\text{bcp}}$	+0.454	+0.034	+0.444	+0.025
V_{bcp}^a	-0.22450	-0.00521	-0.21573	-0.00347
H_{bcp}^b	-0.5667	-0.0170	-0.0553	-0.0014
$ H_{\text{bcp}} /\rho_{\text{bcp}}$	0.42	0.02	0.40	0.02
$ V_{\text{bcp}} /G_{\text{bcp}}$	1.32	0.75	1.32	0.71
DI ^c	1.04	0.04	0.99	0.03
E_{int} , kcal.mol ⁻¹	70.4	1.7	67.7	1.1

^a Potential energy density; ^b Energy density H_{bcp} ; ^c Delocalization index.

type of weak interaction between the CO ligand and the C_{ipso} carbon atom of one of the $P^+-\text{Ph}$ substituents albeit with significantly lower energy (1.1 kcal.mol⁻¹) was also evidenced in the Pd complex $[14c^{2+}]$. All these interactions contribute to the stability of the two pincer Pd(II) complexes of interest, and are in agreement with experimental observations, namely the higher stability of the Pd–CO pincer complex $[4](\text{OTf})$ featuring a central ylide fragment compared to its central NHC analogue $[14c](\text{OTf})_2$.

CONCLUSION

An isostructural family of phosphonium ylide core $[C,C,C\text{-}Pd(L)](\text{OTf})$ ($L = \text{NCMe}, \text{CN}t\text{Bu}, \text{CO}$) pincer complexes was easily prepared by the base-assisted activation of three C–H bonds in a readily available *N*-phosphonio-substituted imidazolium salt as a key step. The complete series of these Pd(II) species was fully characterized including by X-ray diffraction study. The electronic donation of new phosphonium ylide core LX_2 -type pincer scaffold evaluated on the basis of IR spectroscopy, cyclic voltammetry and MOs analysis data, was shown to be higher than for the related $C,C,C\text{-NHC}$, bis(phosphonium ylide) ligand. The extreme electron-rich character of this new pincer platform was found to be beneficial for the structural characterization of a Pd–CO adduct, thereby compensating the absence of strongly donating alkyl ligands typically required for the stabilization of these elusive species. Thanks to the unconventional reactivity observed with (allyl)MgBr and *n*BuLi from cationic precursors, zwitterionic Pd(II) pincer complexes bearing bromide and acyl co-ligands were selectively obtained. The X nature of the *trans* ylide coordinated ligand makes these two Pd(II) complexes unique cases of the restricted family of zwitterionic phosphonium organopalladates where the negative charge initially located at the $C\text{-}sp^3$ ylidic carbon atom is formally transferred to the metal atom and actually partially delocalized over the bromide and acyl fragments. These results illustrate how the nature of the pincer backbone can influence the electronic properties and thus directly impact the reactivity of the ensuing complexes. Application of these carbon-based pincer complexes in homogeneous catalysis and the extension of this approach to other transition metals are currently underway.

EXPERIMENTAL SECTION

General Remarks. All manipulations were performed under an inert atmosphere of dry nitrogen by using standard vacuum line and Schlenk tube techniques. Glassware was dried at 120 °C in an oven for at least three hours. Dry and oxygen-free organic solvents (THF, Et₂O, CH₂Cl₂, toluene, pentane) were obtained using a LabSolv (Innovative Technology) solvent purification system. Acetonitrile was dried and distilled over P₂O₅ under argon. A liquid nitrogen/ethanol slush bath was used to maintain samples at the desired low temperature. 1-mesityl-3-(3-(triphenylphosphonio)propyl)imidazolium trifluoromethane sulfonate $[1](\text{OTf})_2$ was prepared according to a previously described procedure.¹⁶ All other reagent-grade chemicals were purchased from commercial sources and used as received. Chromatographic purification was carried out on silica gel (SiO₂, 63–200 μm). Solution IR spectra were recorded in 0.1 mm CaF₂ cells with 0.5 cm⁻¹ resolution using a Perkin Elmer Frontier FT-IR spectrometer and given in cm⁻¹ with relative intensity in parentheses. ¹H, ³¹P, and ¹³C NMR spectra were obtained on Bruker AV300, AV400 or NEO600 spectrometers. NMR chemical shifts δ are in ppm, with positive values to high frequency referenced against the residual signals of deuterated solvents for ¹H and ¹³C and 85% H₃PO₄ for ³¹P. If necessary, additional information on the carbon signal attribution was obtained using ¹³C{¹H, ³¹P}, *J*-modulated spin-echo (JMOD) ¹³C{¹H}, ¹H–¹³C HMQC, and/or HMBC experiments. MS spectra (ESI mode) were performed by the

mass spectrometry service of the “Institut de Chimie de Toulouse” using a Xevo G2 QToF (Waters) spectrometer. Elemental analyses were carried out by the elemental analysis service of the “LCC” using a Perkin Elmer 2400 series II analyzer. Voltammetric measurements were performed by the electrochemistry service of the “LCC”.

Voltammetric measurements were carried out with a potentiostat Autolab PGSTAT100 controlled by GPES 4.09 software. Experiments were performed at room temperature in a homemade airtight three-electrode cell consisting of a Pt working electrode ($d = 0.5$ mm), a platinum wire ($S = 1$ cm²) as counter electrode, and a saturated calomel electrode (SCE) separated from the solution by a bridge compartment as a reference. Before each measurement, the working electrode was cleaned with a polishing machine (Presi P230, P4000). The measurements were carried out in dry CH₂Cl₂ under argon atmosphere using 0.1 M [*n*Bu₄N](OTf) (Fluka, 99% puriss electrochemical grade) as supporting electrolyte and typically 10⁻³ M concentration of Pd(II) complexes [2-4](OTf).

Synthesis of complex [2](OTf). A mixture of [1](OTf)₂ (0.8 g, 1.0 mmol), PdCl₂ (0.17 g, 1.0 mmol), and anhydrous Cs₂CO₃ (1.6 g, 5.0 mmol) was stirred at 70 °C in CH₃CN (8 mL) for 16 hours. After filtration over celite and evaporation of the solvent under vacuum, the crude residue was dissolved in CH₂Cl₂ (10 mL), and the solution was filtered over Celite. Purification by chromatography on silica gel (AcOEt/MeOH) gave [2](OTf) as a beige powder (0.63 g, 80%). Recrystallization from CH₂Cl₂/Et₂O at room temperature gave colorless crystals, some of them being suitable for X-Ray diffraction experiment. ¹H NMR (600 MHz, CD₃CN, 25 °C): $\delta = 7.78$ – 7.75 (m, 1H, CH_{Ar}), 7.71–7.63 (m, 6H, CH_{Ar}), 7.59–7.53 (m, 4H, CH_{Ar}), 7.26–7.24 (m, 1H, CH_{Ar}), 7.21 (brs, 1H, CH_{Ar}), 7.14–7.10 (m, 1H, CH_{Ar}), 7.07–7.03 (m, 2H, CH_{Ar}), 6.93 (brs, 1H, CH_{Ar}), 6.86 (brs, 1H, CH_{Ar}), 4.11–4.07 (m, 1H, NCH₂), 4.03–3.99 (m, 1H, NCH₂), 3.54–3.49 (m, 1H, PCH), 2.31 (s, 3H, CH_{3Mes}), 2.13–2.08 (m, 1H, CH₂), 2.07 (s, 3H, CH_{3Mes}), 1.80–1.73 (m, 1H, CH₂), 1.49 (s, 3H, CH_{3Mes}); ³¹P{¹H} NMR (243 MHz, CD₃CN, 25 °C): $\delta = 33.5$ (s); ¹³C NMR (151 MHz, CD₃CN, 25 °C): $\delta = 176.6$ (d, $J_{CP} = 5.5$ Hz, N₂C), 175.2 (d, $J_{CP} = 33.9$ Hz, C_{Ph}), 139.9 (s, C_{Mes}), 137.8 (d, $J_{CP} = 19.4$ Hz, CH_{Ph}), 137.5 (s, C_{Mes}), 136.6 (s, C_{Mes}), 136.2 (s, C_{Mes}), 136.0 (d, $J_{CP} = 119.7$ Hz, C_{Ph}), 134.7 (d, $J_{CP} = 9.1$ Hz, CH_{Ph}), 134.5 (s, CH_{Ph}), 134.0 (s, CH_{Ph}), 133.9 (d, $J_{CP} = 9.4$ Hz, CH_{Ph}), 131.0 (s, CH_{Ph}), 130.9 (d, $J_{CP} = 3.2$ Hz, CH_{Ph}), 130.7 (d, $J_{CP} = 10.7$ Hz, CH_{Ph}), 130.2 (d, $J_{CP} = 11.9$ Hz, CH_{Ph}), 129.9 (s, CH_{Ph}), 129.7 (s, CH_{Ph}), 126.4 (d, $J_{CP} = 89.1$ Hz, C_{Ph}), 126.1 (d, $J_{CP} = 12.7$ Hz, CH_{Ph}), 125.6 (d, $J_{CP} = 58.7$ Hz, C_{Ph}), 123.2 (s, CH_{Ph}), 122.9 (s, CH_{Ph}), 121.3 (q, $J_{CF} = 321.0$ Hz, CF₃), 53.3 (d, $J_{CP} = 20.0$ Hz, NCH₂), 27.3 (s, CH₂), 21.0 (s, CH_{3Mes}), 19.5 (d, $J_{CP} = 43.3$ Hz, PCH), 18.0 (s, CH_{3Mes}), 17.9 (s, CH_{3Mes}); MS (ES⁺): m/z : 634.2 [M – CF₃SO₃]⁺; HRMS (ES⁺): calcd for C₃₅H₃₅N₃PPd, 634.1603; found, 634.1619 ($\epsilon_r = 2.5$ ppm). Elemental analysis for C₃₆H₃₅F₃N₃O₃PPdS: calcd, C 55.14, H 4.50, N 5.36; found, C 54.63, H 4.44, N 5.23.

Synthesis of complex [3](OTf). *t*-Butyl isocyanide (21.6 μ L, 0.19 mmol) was added at –78 °C to a solution of complex [2](OTf) (0.1 g, 0.13 mmol) in CH₂Cl₂ (10 mL). The mixture was warmed to room temperature and stirred for 2 hours. After filtration over Celite, the solvent was removed under vacuum. After washing with Et₂O (10 mL), complex [3](OTf) was obtained as a pale yellow powder (0.099 g, 94%). Recrystallization from CH₂Cl₂/Et₂O at –20 °C gave colorless crystals, some of them being suitable for X-Ray diffraction experiment. ¹H NMR (600 MHz, CD₂Cl₂, 25 °C) $\delta = 7.76$ – 7.74 (m, 2H, CH_{Ar}), 7.69–7.65 (m, 5H, CH_{Ar}), 7.59–7.51 (m, 4H, CH_{Ar}), 7.27–7.24 (m, 1H, CH_{Ar}), 7.19 (d, $J_{HH} = 1.8$ Hz, 1H, CH_{Ar}), 7.14–7.10 (m, 1H, CH_{Ar}), 7.08–7.05 (m, 1H, CH_{Ar}), 7.03 (brs, 1H, CH_{Ar}), 6.92 (brs, 1H, CH_{Ar}), 6.79 (d, $J_{HH} = 1.8$ Hz, 1H, CH_{Ar}), 4.02–3.98 (m, 1H, NCH₂), 3.83–3.80 (m, 1H, NCH₂), 3.16–3.11 (m, 1H, PCH), 2.35 (s, 3H, CH_{3Mes}), 2.30–2.23 (m, 1H, CH₂), 2.12 (s, 3H, CH_{3Mes}), 2.01–1.93 (m, 1H, CH₂), 1.55 (s, 3H, CH_{3Mes}), 1.35 (s, 9H, C(CH₃)₃); ³¹P{¹H} NMR (243 MHz, CD₂Cl₂, 25 °C): $\delta = 33.5$ (s); ¹³C NMR (151 MHz, CD₂Cl₂, 25 °C): $\delta = 176.4$ (d, $J_{CP} = 6.1$ Hz, N₂C), 172.5 (d, $J_{CP} = 32.6$ Hz, C_{Ph}), 140.1 (d, $J_{CP} = 18.1$ Hz, CH_{Ph}), 139.3 (s, C_{Mes}), 138.4 (brs, C_{CN}), 136.8 (s, C_{Mes}), 136.4 (d, $J_{CP} = 114.2$ Hz, C_{Ph}), 135.8 (s, C_{Mes}), 135.4 (s, C_{Mes}), 134.1 (d, $J_{CP} = 9.3$ Hz, CH_{Ph}), 133.8 (s, CH_{Ph}), 133.4 (s, CH_{Ph}), 133.3 (d, $J_{CP} = 9.3$ Hz, CH_{Ph}), 131.3 (d, $J_{CP} = 18.4$ Hz, CH_{Ph}), 130.5 (d, $J_{CP} = 3.2$ Hz, CH_{Ph}), 130.2 (d, $J_{CP} = 10.7$ Hz, CH_{Ph}), 129.9 (s, CH_{Ph}), 129.8 (d, $J_{CP} =$

12.0 Hz, CH_{Ph}), 129.7 (s, CH_{Ph}), 126.0 (d, $J_{CP} = 86.8$ Hz, C_{Ph}), 125.5 (d, $J_{CP} = 12.7$ Hz, CH_{Ph}), 125.3 (d, $J_{CP} = 58.7$ Hz, C_{Ph}), 122.7 (s, CH_{Ph}), 122.5 (d, $J_{CP} = 5.7$ Hz, CH_{Ph}), 121.4 (q, $J_{CF} = 321.0$ Hz, CF₃), 58.0 (s, C(CH₃)₃), 53.4 (d, $J_{CP} = 15.1$ Hz, NCH₂), 30.1 (s, (CH₃)₃), 26.3 (s, CH₂), 22.3 (d, $J_{CP} = 40.3$ Hz, PCH), 21.2 (s, CH_{3Mes}), 18.6 (s, CH_{3Mes}), 18.1 (s, CH_{3Mes}); IR (CH₂Cl₂): ν_{CN} 2187 cm⁻¹ (s); MS (ES⁺): m/z : 676.2 [M – CF₃SO₃]⁺; HRMS (ES⁺): calcd for C₃₈H₄₁N₃PPd, 676.2073; found, 676.2092 ($\epsilon_r = 2.8$ ppm). Elemental analysis for C₃₉H₄₁F₃N₃O₃PPdS.0.4(CH₂Cl₂): calcd, C 55.01, H 4.90, N 4.89; found, C 55.13, H 4.78, N 4.88.

Synthesis of complex [4](OTf). Complex [2](OTf) (0.15 g, 0.19 mmol) was dissolved in CH₂Cl₂ (5 mL), and carbon monoxide was bubbled during 15 min. at room temperature. A full conversion was observed by ³¹P NMR spectroscopy of the aliquot. After filtration over Celite, the solvent was removed under vacuum, and complex [4](OTf) was obtained as pale yellow powder (0.15 g, 99%). Recrystallization from CH₂Cl₂/Pentane at –20 °C gave colorless crystals suitable for X-Ray diffraction experiment. ¹H NMR (600 MHz, CD₂Cl₂, 25 °C): $\delta = 7.81$ – 7.78 (m, 1H, CH_{Ar}), 7.72–7.68 (m, 6H, CH_{Ar}), 7.55–7.51 (m, 4H, CH_{Ar}), 7.39 (d, $J_{HH} = 1.8$ Hz, 1H, CH_{Ar}), 7.34–7.31 (m, 1H, CH_{Ar}), 7.23–7.19 (m, 1H, CH_{Ar}), 7.15–7.12 (m, 1H, CH_{Ar}), 7.06 (brs, 1H, CH_{Ar}), 6.94 (d, $J_{HH} = 1.9$ Hz, 2H, CH_{Ar}), 4.36–4.34 (m, 1H, NCH₂), 4.19–4.14 (m, 1H, NCH₂), 3.46–3.41 (m, 1H, PCH), 2.48–2.44 (m, 1H, CH₂), 2.35 (s, 3H, CH_{3Mes}), 2.06 (s, 3H, CH_{3Mes}), 1.96–1.89 (m, 1H, CH₂), 1.38 (s, 3H, CH_{3Mes}); ³¹P{¹H} NMR (243 MHz, CD₂Cl₂, 25 °C): $\delta = 35.8$ (s); ¹³C NMR (151 MHz, CD₂Cl₂, 25 °C): $\delta = 180.5$ (d, $J_{CP} = 5.9$ Hz, CO), 174.0 (d, $J_{CP} = 5.1$ Hz, N₂C), 169.2 (d, $J_{CP} = 31.1$ Hz, C_{Ph}), 141.1 (s, C_{Mes}), 140.6 (d, $J_{CP} = 18.9$ Hz, CH_{Ph}), 136.6 (s, C_{Mes}), 136.1 (s, C_{Mes}), 135.9 (s, C_{Mes}), 135.4 (d, $J_{CP} = 113.4$ Hz, C_{Ph}), 134.4 (d, $J_{CP} = 2.8$ Hz, CH_{Ph}), 134.1 (d, $J_{CP} = 9.1$ Hz, CH_{Ph}), 133.8 (d, $J_{CP} = 3.0$ Hz, CH_{Ph}), 133.4 (d, $J_{CP} = 9.9$ Hz, CH_{Ph}), 131.9 (d, $J_{CP} = 18.2$ Hz, CH_{Ph}), 131.7 (d, $J_{CP} = 3.2$ Hz, CH_{Ph}), 130.4 (d, $J_{CP} = 11.0$ Hz, CH_{Ph}), 130.0 (s, CH_{Ph}), 129.9 (d, $J_{CP} = 12.1$ Hz, CH_{Ph}), 129.8 (s, CH_{Ph}), 126.6 (d, $J_{CP} = 12.5$ Hz, CH_{Ph}), 124.9 (d, $J_{CP} = 90.6$ Hz, C_{Ph}), 124.0 (d, $J_{CP} = 58.7$ Hz, C_{Ph}), 123.9 (s, CH_{Ph}), 122.2 (s, CH_{Ph}), 121.5 (q, $J_{CF} = 321.6$ Hz, CF₃), 53.8 (d, $J_{CP} = 15.1$ Hz, NCH₂), 27.9 (d, $J_{CP} = 43.3$ Hz, PCH), 26.1 (s, CH₂), 21.2 (s, CH_{3Mes}), 17.8 (s, CH_{3Mes}), 17.5 (s, CH_{3Mes}); IR (CH₂Cl₂): ν_{CO} 2105 cm⁻¹ (s); MS (ES⁺): m/z : 621.1 [M – CF₃SO₃]⁺; HRMS (ES⁺): calcd for C₃₄H₃₂N₂OPPd, 621.1300; found, 621.1309 ($\epsilon_r = 1.4$ ppm).

Synthesis of complex 5. A solution of (allyl)MgBr (1 M in Et₂O, 89 μ L, 0.09 mmol) was added at 0 °C to a solution of complex [2](OTf) (0.07 g, 0.09 mmol) in THF (5 mL). The mixture was warmed to room temperature and stirred for 2 hours. After evaporation of the solvent under vacuum, the crude residue was dissolved in CH₂Cl₂ (5 mL), and the solution was filtered over Celite. Recrystallization from CH₂Cl₂/Et₂O at –20 °C gave complex 5 as a white powder (0.04 g, 72%). Single crystals suitable for XRD were obtained in a concentrated solution of CH₂Cl₂ at –20 °C. ¹H NMR (600 MHz, CD₂Cl₂, 25 °C): $\delta = 8.53$ (d, $J_{HH} = 6.0$ Hz, 1H, CH_{Ar}), 7.71–7.60 (m, 8H, CH_{Ar}), 7.51–7.48 (m, 2H, CH_{Ar}), 7.13 (t, $J_{HH} = 6.0$ Hz, 1H, CH_{Ar}), 6.97–6.89 (m, 4H, CH_{Ar}), 6.82 (brs, 1H, CH_{Ar}), 6.63 (brs, 1H, CH_{Ar}), 3.91–3.87 (m, 1H, NCH₂), 3.57–3.53 (m, 1H, NCH₂), 3.40–3.37 (m, 1H, PCH), 2.32 (s, 3H, CH_{3Mes}), 2.17 (s, 3H, CH_{3Mes}), 2.08–1.91 (m, 2H, CH₂), 1.69 (s, 3H, CH_{3Mes}); ³¹P{¹H} NMR (243 MHz, CD₂Cl₂, 25 °C): $\delta = 29.8$ (s); ¹³C NMR (151 MHz, CD₂Cl₂, 25 °C): $\delta = 181.7$ (d, $J_{CP} = 6.0$ Hz, N₂C), 178.0 (d, $J_{CP} = 33.2$ Hz, C_{Ph}), 141.2 (d, $J_{CP} = 19.6$ Hz, CH_{Ph}), 138.1 (s, C_{Mes}), 137.8 (s, C_{Mes}), 135.7 (s, C_{Mes}), 135.6 (s, C_{Mes}), 135.6 (d, $J_{CP} = 116.3$ Hz, C_{Ph}), 134.6 (d, $J_{CP} = 9.1$ Hz, CH_{Ph}), 132.3 (d, $J_{CP} = 9.1$ Hz, CH_{Ph}), 133.1 (s, CH_{Ph}), 132.8 (s, CH_{Ph}), 129.8 (d, $J_{CP} = 9.1$ Hz, CH_{Ph}), 129.6 (s, CH_{Ph}), 129.4 (d, $J_{CP} = 9.1$ Hz, CH_{Ph}), 129.2 (d, $J_{CP} = 19.6$ Hz, CH_{Ph}), 128.7 (s, CH_{Ph}), 127.1 (d, $J_{CP} = 84.6$ Hz, C_{Ph}), 126.9 (d, $J_{CP} = 55.9$ Hz, C_{Ph}), 124.0 (d, $J_{CP} = 13.6$ Hz, CH_{Ph}), 122.7 (s, CH_{Ph}), 120.6 (s, CH_{Ph}), 53.2 (d, $J_{CP} = 12.1$ Hz, NCH₂), 27.5 (s, CH₂), 21.2 (s, CH_{3Mes}), 19.2 (s, CH_{3Mes}), 18.7 (d, $J_{CP} = 42.3$ Hz, PCH), 18.6 (s, CH_{3Mes}); MS (ES⁺): m/z : 593.1 [M – Br]⁺; HRMS (ES⁺): calcd for C₃₃H₃₂N₂PPd, 593.1350; found, 593.1359 ($\epsilon_r = 1.5$ ppm). Elemental analysis for C₃₃H₃₂BrN₂PPd.1.3(CH₂Cl₂): calcd, C 52.53, H 4.45, N 3.57; found, C 52.29, H 4.56, N 4.19.

Synthesis of complex 6. A solution of *n*BuLi (2.5 M in hexane, 55 μ L, 0.15 mmol) was added at –78 °C to a solution of complex [4](OTf) (0.1

g, 0.13 mmol) in THF (10 mL). The mixture was warmed to room temperature and stirred for 2 hours. After evaporation of the solvent under vacuum, the crude residue was dissolved in CH₂Cl₂ (5 mL), and the solution was filtered over Celite. Recrystallization from CH₂Cl₂/Et₂O at -20 °C gave complex **6** as a white powder (0.07 g, 81%). ¹H NMR (400 MHz, THF-*d*₈, 25 °C): (The ¹H NMR resonance of the PCH fragment was not observed): δ = 7.71–7.67 (m, 2H, CH_{Ar}), 7.57–7.50 (m, 6H, CH_{Ar}), 7.42–7.36 (m, 3H, CH_{Ar}), 7.15 (brs, 1H, CH_{Ar}), 6.91 (t, *J*_{HH} = 8.0 Hz, 1H, CH_{Ar}), 6.79–6.72 (m, 4H, CH_{Ar}), 6.57 (brs, 1H, CH_{Ar}), 4.10–3.93 (m, 1H, NCH₂), 3.85–3.79 (m, 1H, NCH₂), 2.40–2.30 (m, 2H, CH₂), 2.20 (s, 3H, CH_{3Mes}), 1.96 (s, 3H, CH_{3Mes}), 1.85–1.75 (m, 1H, CH₂), 1.33 (s, 3H, CH_{3Mes}), 1.25–1.10 (m, 3H, CH₂), 0.95–0.80 (m, 2H, CH₂), 0.71 (t, *J*_{HH} = 8.0 Hz, 3H, CH₃); ³¹P{¹H} NMR (162 MHz, THF-*d*₈, 25 °C): δ = 18.8 (s); ¹³C NMR (101 MHz, THF-*d*₈, 25 °C): δ = 277.1 (brs, CO), 183.3 (d, *J*_{CP} = 6.1 Hz, N₂C), 181.3 (d, *J*_{CP} = 31.3 Hz, C_{Ph}), 140.5 (d, *J*_{CP} = 19.2 Hz, CH_{Ph}), 139.9 (d, *J*_{CP} = 119.2 Hz, C_{Ph}), 138.7 (s, C_{Mes}), 138.4 (s, C_{Mes}), 137.2 (s, C_{Mes}), 136.9 (s, C_{Mes}), 135.0 (d, *J*_{CP} = 9.1 Hz, CH_{Ph}), 133.9 (d, *J*_{CP} = 9.1 Hz, CH_{Ph}), 132.5 (d, *J*_{CP} = 3.0 Hz, CH_{Ph}), 132.2 (d, *J*_{CP} = 3.0 Hz, CH_{Ph}), 132.2 (d, *J*_{CP} = 47.5 Hz, C_{Ph}), 130.7 (d, *J*_{CP} = 92.9 Hz, C_{Ph}), 130.7 (d, *J*_{CP} = 10.0 Hz, CH_{Ph}), 130.0 (s, CH_{Ph}), 129.9 (d, *J*_{CP} = 11.1 Hz, CH_{Ph}), 129.3 (d, *J*_{CP} = 11.1 Hz, CH_{Ph}), 129.2 (d, *J*_{CP} = 3.0 Hz, CH_{Ph}), 129.1 (s, CH_{Ph}), 123.2 (d, *J*_{CP} = 15.1 Hz, CH_{Ph}), 123.0 (s, CH_{Ph}), 121.3 (s, CH_{Ph}), 58.7 (s, COCH₂), 55.8 (d, *J*_{CP} = 22.2 Hz, NCH₂), 27.8 (s, CH₂), 26.8 (s, CH₂), 23.8 (s, CH₂), 21.3 (s, CH₃), 18.7 (s, CH₃), 18.2 (s, CH₃), 17.5 (brd, *J*_{CP} = 43.4 Hz, PCH), 15.0 (s, CH₃); IR (THF): ν_{C=O} 1607 cm⁻¹ (s); MS (ES⁺): *m/z*: 677.2 [M - H]⁺; HRMS (ES⁺): calcd for C₃₈H₄₀N₂OPPd, 677.1913; found, 677.1917 (ε_r = 0.6 ppm).

Single-crystal X-ray diffraction analyses for complexes [2-4](OTf) and **5.** Intensity data were collected at low temperature on an Apex2 Bruker diffractometer equipped with a 30W air-cooled microfocus MoKα source (λ = 0.71073 Å, graphite monochromator). The structures were solved using SUPERFLIP⁴⁵ and refined by means of least-squares procedures using the programs of the PC version of CRYSTALS.⁴⁶ Absorption corrections were introduced using the program MULTISCAN.⁴⁷ Atomic scattering factors were taken from the international tables for X-ray crystallography. All non-hydrogen atoms were refined anisotropically. The H atoms were located in a difference map, but those attached to carbon atoms were repositioned geometrically using a “riding” model. In case of complex [4](OTf), the triflate anion was found to be disordered over two positions with 60:40 occupancy ratio. After the initial step of structural refinement for complex **5**, co-crystallized solvents likely to be severely disordered CH₂Cl₂ and H₂O in partial occupancies were located. Since all attempts to refine them as discrete molecules did not afford a satisfactory model, it was decided to remove their contribution using Squeeze procedure⁴⁸ (total number of electrons in one unit cell is 134 electrons, total accessible void is 193 Å³). Additional experimental details and refinement parameters are given in Table S1.

Computational details. Geometries were fully optimized at the PBE-D3/6-31G**/LANL2DZ* (Pd) level of calculation using Gaussian 09.⁴⁹ The star in LANL2DZ*(Pd) refers to *f*-polarization functions derived by Ehlers *et al.* for Pd,⁵⁰ that have been added to the LANL2DZ(Pd) basis set. Vibrational analysis was performed at the same level as the geometry optimization in order to check the obtention of a minimum on the potential energy surface. QTAIM analysis was performed with the AIMAll software.⁵¹ Topological methods are based on the analysis of the gradient field of a local function within the dynamic field theory and provide a partition of the molecular space into non-overlapping basins. The topological analysis of the electron density ρ(*r*), designed as the Quantum Theory of Atoms in Molecules (QTAIM) by Bader, yields atomic basins and QTAIM atomic charges.⁵² It allows defining bond paths and bond critical points (BCPs). The nature of the chemical bond is characterized from various properties of the electron density at the BCPs, especially the sign of the Laplacian of the electron density and the values of the kinetic energy density (*G*_{bcp}), of the potential energy density (*V*_{bcp}) and of the energy density *H*_{bcp} = *G*_{bcp} + *V*_{bcp}, following the Bianchi's⁴⁰ and Macchi's classification.⁴¹ Negative and positive values for the Laplacian of the electron density at the BCP are assigned to « electron-shared » and « closed-shell » interactions, respectively.⁵² Bianchi *et al.* distinguish

three bonding regimes, depending on the value of the absolute ratio of the potential energy density to the kinetic energy density ($|V_{bcp}|/G_{bcp}$). The intermediate bond regime ($1 < |V_{bcp}|/G_{bcp} < 2$) lies between electron-shared covalent bonds ($|V_{bcp}|/G_{bcp}$ greater than 2) and closed-shell ionic bonds or van der Waals interactions ($|V_{bcp}|/G_{bcp}$ lower than 1) and includes dative bonds and ionic bonds of weak covalent character. The Macchi's classification relies on the values of both local descriptors and the delocalization index (DI) and offers a way to refine the bond characterization further. The covalence degree may be estimated from the latter and from $|H_{bcp}|/\rho_{bcp}$. The strength of the interaction may be estimated from the correlation scheme of Espinosa *et al.*⁴² providing the corresponding positive interaction energy ($E_{int} = -1/2 V_{bcp}$), with E_{int} (kcal.mol⁻¹) = -313.754 × *V*_{bcp} (a.u.).

ASSOCIATED CONTENT

Supporting Information

The Supporting Information is available free of charge on the ACS Publications website.

¹H, ³¹P and ¹³C NMR for all new compounds, solution IR spectra for complexes [3-4](OTf), cyclic voltammograms for complexes [2-4](OTf) and additional crystallographic data for complexes [2-4](OTf) and **5** (PDF).

Optimized structures of pincer Pd(II) complexes **2**⁺, **3**⁺, **4**⁺, and **14c**²⁺ (PDF and xyz files).

AUTHOR INFORMATION

Corresponding Authors

* E-mail for D.A.V.: dmitry.valyaev@lcc-toulouse.fr

* E-mail for Y.C.: yves.canac@lcc-toulouse.fr

ORCID

Christine Lepetit: 0000-0002-0008-9506

Dmitry A. Valyaev: 0000-0002-1772-844X

Yves Canac: 0000-0002-3747-554X

Notes

The authors declare no competing financial interest.

ACKNOWLEDGMENT

The authors thank the Centre National de la Recherche Scientifique (CNRS) for financial support, Alix Saquet for electrochemistry experiments, and Dr A. Auffrant for helpful discussions. R. T. is grateful to French MENESR for a PhD fellowship. Computational studies were performed using HPC resources from CALMIP (Grant 2020-2021 [0851]) and from GENCI-[CINES/IDRIS] (Grant 2020-2021 [085008]).

REFERENCES

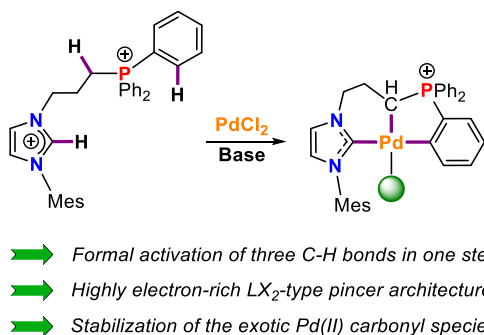
- (1) Moulton, C. J.; Shaw, B. L. Transition metal-carbon bonds. Part XLII. Complexes of nickel, palladium, platinum, rhodium and iridium with the tridentate ligand 2,6-bis[(di-*t*-butylphosphino)methyl]phenyl. *J. Chem. Soc. Dalton Trans.* **1976**, 1020–1024.
- (2) (a) van Koten, G. Tuning the reactivity of metals held in a rigid ligand environment. *Pure Appl. Chem.* **1989**, *61*, 1681–1694. (b) Benito-Garagorri, D.; Kirchner, K. Modularly designed transition metal PNP and PCP pincer complexes based on aminophosphines: synthesis and catalytic applications. *Acc. Chem. Res.* **2008**, *41*, 201–203. (c) Morales-Morales, D.; Jensen, C. G. M. *The Chemistry of Pincer Compounds*, Elsevier Science: **2011**. (d) Van Koten, G.; Milstein, D. *Organometallic Pincer Chemistry*, Eds. Van Koten, G.; Milstein, D. *Top. Organomet. Chem.* **2013**, *40*, 1–356; Springer-Verlag Berlin Heidelberg. (e) Roddick, D. M.; Zargarian, D. Pentacoordination for pincer and related terdentate coordination compounds: revisiting structural properties and trends for d⁸ transition metal systems. *Inorg. Chim. Acta* **2014**, *422*, 251–264.

- (3) (a) Pincer and pincer-type complexes: applications in organic synthesis and catalysis, Eds. Szabó, K. J.; Wendt, O. F. Wiley-VCH, Weinheim, Germany, **2014**. (b) Gunanathan, G.; Milstein, D. Bond activation and catalysis by ruthenium pincer complexes. *Chem. Rev.* **2014**, *114*, 12024–12087. (c) Asay, M.; Morales-Morales, D. Non-symmetric pincer ligands: complexes and applications in catalysis. *Dalton Trans.* **2015**, *44*, 17432–17447. (d) Adams, G. M.; Weller, A. S. POP-type ligands: variable coordination and hemilabile behaviour. *Coord. Chem. Rev.* **2018**, *355*, 150–172. (e) Maser, L.; Vondung, L.; Langer, R. The ABC in pincer chemistry – from amine to borylene and carbon-based pincer ligands. *Polyhedron*, **2018**, *143*, 28–42. (f) Wang, Y.; Zhang, B.; Guo, S. Transition metal complexes supported by N-heterocyclic carbene-based pincer platforms: synthesis, reactivity and applications. *Eur. J. Inorg. Chem.* **2021**, *2021*, 188–204.
- (4) (a) Maaliki, A.; Lepetit, C.; Canac, Y.; Bijani, C.; Duhayon, C.; Chauvin, R. On the P-coordinating limit of NHC-phosphenium cations towards Rh^I centers. *Chem. Eur. J.* **2012**, *18*, 7705–7714. (b) Canac, Y.; Maaliki, C.; Abdellah, I.; Chauvin, R. Carbeniophosphines and their carbon → phosphorus → metal ternary complexes. *New J. Chem.* **2012**, *36*, 17–27. (c) Canac, Y. Carbeniophosphines versus phosphinocarbenes: The role of the positive charge. *Chem. Asian. J.* **2018**, *13*, 1872–1887.
- (5) (a) Canac, Y.; Chauvin, R. Atropochiral C,X- and C,C-chelating carbon ligands. *Eur. J. Inorg. Chem.* **2010**, 2325–2335. (b) Canac, Y.; Lepetit, C.; Chauvin, R. Neutral η¹-carbon ligands: Beyond carbon monoxide. *Top. Organomet. Chem.* Chauvin, R.; Canac, Y. Eds, Springer, **2010**, *30*, 1–12. (c) Taakili, R. Canac, Y. NHC core pincer ligands exhibiting two anionic coordinating extremities. *Molecules* **2020**, *25*, 2231.
- (6) (a) Gründemann, S.; Albrecht, M.; Loch, J. A.; Faller, J. W.; Crabtree, R. H. Tridentate carbene CCC and CNC pincer palladium(II) complexes: structure, fluxionality, and catalytic activity. *Organometallics*, **2001**, *20*, 5485–5488. (b) Rubio, R. J.; Andavan, G. T. S.; Bauer, E. B.; Hollis, T. K.; Cho, J.; Tham, F. S.; Donnadiou, B. Toward a general method for CCC N-heterocyclic carbene pincer synthesis: metallation and transmetallation strategies for concurrent activation of three C–H bonds. *J. Organomet. Chem.* **2005**, *690*, 5353–5364. (c) Denny, J. A.; Lang, G. M.; Hollis, T. K. CCC-NHC pincer complexes: synthesis, applications, and catalysis. *Pincer Compounds* Morales-Morales, D. Ed, Elsevier, **2018**, 251–272.
- (7) (a) Eguillor, B.; Esteruelas, M. A.; Lezáun, V.; Oliván, M.; Oñate, E.; Tsai, J.-Y.; Xia, C. A capped octahedral MHC₆ compound of a platinum group metal. *Chem. Eur. J.* **2016**, *22*, 9106–9110. (b) Yan, Z.-B.; Dai, K.-L.; Yang, B.-M.; Li, Z.-H.; Tu, Y.-Q.; Zhang, F.-M.; Zhang, X.-M.; Peng, M.; Chen, Q.-L.; Jing, Z.-R. Development of unique dianionic Ir(III) CCC pincer complexes with a favourable spirocyclic NHC framework. *Sci. China Chem.* **2020**, *63*, 1761–1766.
- (8) (a) Kubo, K.; Jones, N. D.; Ferguson, M. J.; McDonald, R.; Cavell, R. G. Chelate and pincer carbene complexes of rhodium and platinum derived from hexaphenylcarbodiphosphorane, Ph₃P=C=PPh₃. *J. Am. Chem. Soc.* **2005**, *127*, 5314–5315. (b) Petz, W.; Neumüller, B. New platinum complexes with carbodiphosphorane as pincer ligand via ortho phenyl metallation. *Polyhedron*, **2011**, *30*, 1779–1784. (c) Kubo, K.; Okitsu, H.; Miwa, H.; Kume, S.; Cavell, R. G. Carbon(0)-bridged Pt/Ag dinuclear and tetranuclear complexes based on a cyclometalated pincer carbodiphosphorane platform. *Organometallics*, **2017**, *36*, 266–274.
- (9) (a) Paulose, T. A. P.; Wu, S.-C.; Quail, J. W.; Foley, S. R. Synthesis, characterization and properties of a tri(N-heterocyclic carbene) palladium(II) complex. *Inorg. Chem. Commun.* **2012**, *15*, 37–39. (b) Seo, C.; Cheong, Y.-J.; Yoon, W.; Kim, J.; Shin, J.; Yun, H.; Kim, S.-J.; Jang, H.-Y. Mononuclear copper complexes with tridentate tris(N-heterocyclic carbene): synthesis and catalysis of alkyne-azide cycloaddition. *Organometallics* **2021**, *40*, 16–22.
- (10) Sattler, A.; Parkin, G. A new class of transition metal pincer ligand: tantalum complexes that feature a [CCC] X₃-donor array derived from a terphenyl ligand. *J. Am. Chem. Soc.* **2012**, *134*, 2355–2366.
- (11) (a) Bourissou, D.; Guerret, O.; Gabbai, F. P.; Bertrand, G. Stable carbenes. *Chem. Rev.* **2000**, *100*, 39–91. (b) Y. Canac, M. Soleilhavoup, S. Conejero, G. Bertrand, Stable non-N-heterocyclic carbenes (non-NHC): recent progress. *J. Organomet. Chem.* **2004**, *689*, 3857–3865. (c) Melaimi, M.; Soleilhavoup, M.; G. Bertrand, G. Stable carbenes and related species beyond diaminocarbenes. *Angew. Chem. Int. Ed.* **2010**, *49*, 8810–8849. (d) Hopkinson, M. N.; Richter, C.; Schedler, M.; Glorius, F. An overview of N-Heterocyclic carbenes. *Nature* **2014**, *510*, 485–496. (e) Vivancos, A.; Segarra, C.; Albrecht, M. Mesoionic and related less heteroatom-stabilized N-heterocyclic carbene complexes: synthesis, catalysis, and other applications. *Chem. Rev.* **2018**, *118*, 9493–9586. (f) Sau, S. C.; Hota, P. K.; Mandal, S. K.; Soleilhavoup, M.; Bertrand, G. Stable abnormal N-heterocyclic carbenes and their applications. *Chem. Soc. Rev.* **2020**, *49*, 1233–1252.
- (12) (a) Schmidbaur, H. Phosphorus ylides in the coordination sphere of transition metals: an inventory. *Angew. Chem. Int. Ed. Engl.* **1983**, *22*, 907–927. (b) Kaska, W. C.; Ostojka Starzewski, K. A., in: *Ylides and Imines of Phosphorus*; Johnson, A. W., Eds, John Wiley & Sons: New York, **1993**, chapter 14. (c) Kolodiazhyi, O. I. C-element-substituted phosphorus ylides. *Tetrahedron* **1996**, *52*, 1855–1929. (d) Vicente, J. Chicote, M. T. The ‘acac method’ for the synthesis and coordination of organometallic compounds: synthesis of gold complexes. *Coord. Chem. Rev.* **1999**, *193-195*, 1143–1161. (e) Falvello, L. R.; Ginés, J. C.; Carbó, J. J.; Lledós, A.; Navarro, R.; Soler, T.; Urriolabeitia, E. P. Palladium complexes of a phosphorus ylide with two stabilizing groups: synthesis, structure, and DFT study of the bonding modes. *Inorg. Chem.* **2006**, *45*, 6803–6815. (f) Urriolabeitia, E. P. *sp*³-hybridized neutral η¹-carbon ligands. *Top. Organomet. Chem.* Chauvin, R.; Canac, Y. Eds, Springer, **2010**, *30*, 15–48.
- (13) (a) Scherpf, T.; Feichtner, K. S.; Gessner, V. H. Using ylide functionalization to stabilize boron cations. *Angew. Chem. Int. Ed.* **2017**, *56*, 3275–3279. (b) Scharf, L. T.; Gessner, V. H. Metalated ylides: a new class of strong donor ligands with unique electronic properties. *Inorg. Chem.* **2017**, *56*, 8599–8607. (c) Mohapatra, C.; Scharf, L.; Scherpf, T.; Mallick, B.; Feichtner, K.-S.; Schwarz, C.; Gessner, V. H. Isolation of a diylide-stabilized stannylene and germylene: enhanced donor strength coplanar lone pair alignment. *Angew. Chem. Int. Ed.* **2019**, *58*, 7459–7463.
- (14) (a) Maaliki, C.; Abdalilah, M.; Barthes, C.; Duhayon, C.; Canac, Y.; Chauvin, R. Bis-ylide ligands from acyclic proximal diposphonium precursors. *Eur. J. Inorg. Chem.* **2012**, 4057–4064. (b) Serrano, E.; Soler, T.; Urriolabeitia, E. P. Regioselective C-H bond activation of asymmetric bis(ylide)s promoted by Pd. *Eur. J. Inorg. Chem.* **2017**, 2220–2230. (c) Scherpf, T.; Schwarz, C.; Scharf, L. T.; Zur, J.-A.; Helbig, A.; Gessner, V. H. Ylide-functionalized phosphines: strong donor ligands for homogeneous catalysis. *Angew. Chem. Int. Ed.* **2018**, *57*, 12859–12864. (d) Weber, P.; Scherpf, T.; Rodstein, I.; Lichte, D.; Scharf, L. T.; Gooßen, L. J.; Gessner, V. H. A highly active ylide-functionalized phosphine for palladium catalyzed aminations of aryl chlorides. *Angew. Chem. Int. Ed.* **2019**, *58*, 3203–3207. (e) Handelman, J.; Babu, C. N.; Steinert, H.; Schwarz, C.; Scherpf, T.; Kroll, A.; Gessner, V. H. Towards the rational design of ylide-substituted phosphines for gold(I)-catalysis: from inactive to ppm-level catalysis. *Chem. Sci.* **2021**, *12*, 4329–4337.
- (15) Note that chelating NHC-phosphonium ylide complexes were previously prepared based on a rigid ortho-phenylene bridge, see: (a) Canac, Y.; Duhayon, C.; Chauvin, R. A diaminocarbene-phosphonium ylide: direct access to C,C-chelating ligands. *Angew. Chem. Int. Ed.* **2007**, *46*, 6313–6315. (b) Canac, Y.; Lepetit, C.; Abdalilah, M.; Duhayon, C.; Chauvin, R. Diaminocarbene and phosphonium ylide ligands: a systematic comparison of their donor character. *J. Am. Chem. Soc.* **2008**, *130*, 8406–8413. (c) Abdellah, I.; Debono, N.; Canac, Y.; Duhayon, C.; Chauvin, R. Atropochiral (C,C)-chelating NHC-ylide ligands: synthesis and resolution of palladium(II) complexes thereof. *Dalton Trans.* **2009**, 7196–7202. (d) Canac, Y.; Lepetit, C. Classification of the electronic properties of chelating ligands in *cis*-[LL’Rh(CO)₂] complexes. *Inorg. Chem.* **2017**, *56*, 667–675.
- (16) Benaissa, I.; Taakili, R.; Lugan, N.; Canac, Y. A convenient access to N-phosphonio-substituted NHC metal complexes [M = Ag(I), Rh(I), Pd(II)]. *Dalton Trans.* **2017**, *46*, 12293–12305.
- (17) (a) Taakili, R.; Lepetit, C.; Duhayon, C.; Valyaev, D. A.; Lugan, N.; Canac, Y. Palladium(II) pincer complexes of a C,C,C-NHC, diposphonium bis(ylide) ligand. *Dalton Trans.* **2019**, *48*, 1709–1721. (b) Taakili, R.; Barthes, C.; Goëffon, A.; Lepetit, C.; Duhayon, C.; Val-

- yaev, D. A.; Canac, Y. NHC core phosphonium ylide-based palladium(II) pincer complexes: the second ylide extremity makes the difference. *Inorg. Chem.* **2020**, *59*, 7082–7096.
- (18) Barthes, C.; Bijani, C.; Lukan, N.; Canac, Y. A palladium(II) complex of a C₄ chelating bis(NHC) diphosphonium bis(ylide) ligand. *Organometallics* **2018**, *37*, 673–678.
- (19) One-step synthesis of Pt(II) complexes bearing LX₂-type NHC-amido-aryl pincer ligand has been reported very recently, see: Mell, B.; Rust, J.; Lehmann, C. W.; Berger, R. J. F.; Otte, D.; Ertl, M.; Monkowski, U.; Mohr, F. Arylamidoethyl-functionalized imidazolium salts: precursors for dianionic [C,N,C]²⁻ carbene ligands at a platinum center. *Organometallics* **2021**, *40*, 890–898.
- (20) (a) Delis, J. G. P.; Aubel, P. G.; Vrieze, K.; van Leeuwen, P. W. N. M. Isocyanide insertion into the palladium-carbon bond of complexes containing bidentate nitrogen ligands: a structural and mechanistic study. *Organometallics* **1997**, *16*, 2948–2957. (b) Badaj, A. C.; Lavoie, G. G. Reactivity study of imino-N-heterocyclic carbene palladium methyl complexes. *Organometallics* **2013**, *32*, 4577–4590.
- (21) Jiang, Y.; Zhang, S. Q.; Cao, F.; Zou, J. X.; Yu, J. L.; Shi, B. F.; Hong, X.; Wang, Z. Unexpected stability of CO-coordinated palladacycle in bidentate auxiliary directed C(sp³)-H bond activation: a combined experimental and computational study. *Organometallics*, **2019**, *38*, 2022–2030.
- (22) (a) Liu, J.; Hu, L.; Wang, L.; Chen, H.; Deng, L. An iron(II) ylide complex as a masked open-shell iron alkylidene species in its alkyldiene-transfer reaction with alkenes. *J. Am. Chem. Soc.* **2017**, *139*, 3876–3888. (b) Aleksanyan, D. V.; Churusova, S. G.; Klemenkova, Z. S.; Aysin, R. R.; Rybalkina, E. Y.; Nelyubina, Yu. V.; Artyushin, O. I.; Peregudov, A. S.; Kozlov, V. A. Extending the application scope of organophosphorus(V) compounds in palladium(II) pincer chemistry. *Organometallics* **2019**, *38*, 1062–1080.
- (23) (a) Belluco, U.; Michelin, R. A.; Mozzon, M.; Bertani, R.; Facchin, G.; Zanotto, L.; Pandolfo, L. Functionalized ylides: new trends in organometallic chemistry. *J. Organomet. Chem.* **1998**, *557*, 37–68. (b) Vicente, J.; Chicote, M. T.; MacBeath, C.; Fernández-Baeaa, J.; Baustista, D. Nucleophilic attack of carbonyl-stabilized phosphorus ylides on 1,5-cyclooctadiene complexes on palladium and platinum. *Organometallics* **1999**, *18*, 2677–2682. (c) Adams, R. D.; Smith, M. D.; Wakdikar, N. T. Zwitterionic ammoniumalkenyl ligands in metal cluster complexes. Synthesis, structures, and transformations of zwitterionic trimethylammoniumalkenyl ligands in hexaruthenium carbido carbonyl complexes. *Inorg. Chem.* **2020**, *59*, 1513–1521. (d) Okamoto, K.; Sasakura, K.; Funasaka, S.; Watanabe, H.; Suezaki, M.; Ohe, K. Properties and reactivities of zwitterionic platinum(II)-ate complexes generated by transforming coordination of an alkyne-bisphosphine ligand. *Organometallics* **2021**, *40*, 848–856.
- (24) Solin, N.; Kjellgren, J.; Szabó, K. J. Pincer complex-catalyzed alkylation of aldehyde and imine substrates via nucleophilic η¹-allyl palladium intermediates. *J. Am. Chem. Soc.* **2004**, *126*, 7026–7033.
- (25) Sarbajna, A.; Swamy, V. S. V. S. N.; Gessner, V. H. Phosphorus-ylides: powerful substituents for the stabilization of reactive main group compounds. *Chem. Sci.* **2021**, *12*, 2016–2024.
- (26) Wiessner, T. C.; Asiedu Fosu, S.; Parveen, R.; Rath, N. P.; Vlaisavljevich, B.; Tolman, W. B. Ligand effects on decarbonylation of palladium-acyl complexes. *Organometallics* **2020**, *39*, 3992–3998.
- (27) CCDC 2076949–2076952 contains full crystallographic information for complexes **[2-4]**(OTf) and **5**. These data can be obtained free of charge from the Cambridge Crystallographic Data Centre via www.ccdc.cam.ac.uk/data_request/cif
- (28) Yang, L.; Powell, D. R.; Houser, R. P. Structural variation in copper(I) complexes with pyridylmethylamide ligands: structural analysis with a four-coordinate geometry index, τ_4 . *Dalton Trans.* **2007**, 955–964.
- (29) Bachechi, F. X-ray structural analysis of Ni^{II}, Pd^{II}, and Pt^{II} complexes with the potentially tridentate ligand 1,3-bis(diphenylphosphinomethyl)benzene, 1,3-C₆H₄(CH₂PPh₂)₂. *Struct. Chem.* **2003**, *14*, 263–269.
- (30) (a) Appleton, T. G.; Clark, H. C.; Manzer, L. E. The trans-influence: its measurement and significance. *Coord. Chem. Rev.* **1973**, *10*, 335–422. (b) Anderson, K. M.; Orpen A. G. On the relative magnitudes of *cis* and *trans* influences in metal complexes. *Chem. Commun.* **2001**, 2682–2683 and references therein.
- (31) (a) Sajith, P. K.; Suresh, C. H. Quantification of mutual *trans* influence of ligands in Pd(II) complexes: a combined approach using isodesmic reactions and AIM analysis. *Dalton Trans.* **2010**, *39*, 815–822. (b) Li, Z.; Chifotides, H. T.; Dunbar, K. R. Unprecedented partial paddlewheel dirhodium methylisocyanide compounds with unusual structural and electronic properties: a comprehensive experimental and theoretical study. *Chem. Sci.* **2013**, *4*, 4470–4485.
- (32) García-López, J. A.; Oliva-Madrid, M. J.; Saura-Llamas, I.; Bautista, D.; Vicente, J. Room-temperature isolation of palladium(II) organocarbonyl intermediates in the synthesis of eight-membered lactams after alkyne/CO sequential insertions. *Organometallics*, **2013**, *32*, 1094–1105 and references therein.
- (33) Bolliger, J. L.; Blacque, O.; Frech, C. M. Short, facile, and high-yielding synthesis of extremely efficient pincer-type Suzuki catalysts bearing aminophosphine substituents. *Angew. Chem. Int. Ed.* **2007**, *46*, 6514–6517.
- (34) Lisena, J.; Monot, J.; Mallet-Ladeira, S.; Martin-Vaca, B.; Bourissou, D. Influence of the ligand backbone in pincer complexes: Indenediide, indolyl, and indenyl-based SCS palladium complexes. *Organometallics*, **2013**, *32*, 4301–4305.
- (35) Zucca, A.; Petretto, G. L.; Cabras, M. L.; Stoccoro, S.; Cinellu, M. A.; Manassero, M.; Minghetti, G. N[∧]N[∧]C platinum(II) and palladium(II) cyclometallates of 6,6'-diphenyl-2,2'-bipyridine, L: Crystal and molecular structure of [Pd(L-H)Cl]. *J. Organomet. Chem.* **2009**, *694*, 3753–3761.
- (36) Subramaniam, S. S.; Slaughter, L. M. Direct observation of a carbonylation reaction relevant to CO/alkene copolymerization in a methylpalladium carbonyl complex containing a bis(N-heterocyclic carbene) ligand. *Dalton Trans.* **2009**, 6930–6933.
- (37) (a) Valyaev, D. A.; Brousses, R.; Lukan, N.; Fernández, I.; Sierra, M. A. Do ν(CO) stretching frequencies in metal carbonyl complexes unequivocally correlate with the intrinsic electron-donicity of ancillary ligands? *Chem. Eur. J.* **2011**, *17*, 6602–6605. (b) César, V.; Misal Castro, L. C.; Dombay, T.; Sortais, J.-B.; Darcel, C.; Labat, S.; Miqueu, K.; Sotiropoulos, J.-M.; Brousses, R.; Lukan, N.; Lavigne, G. (Cyclopentadienyl)iron(II) complexes of N-heterocyclic carbenes bearing a malonate or imidate backbone: synthesis, structure, and catalytic potential in hydrosilylation. *Organometallics* **2013**, *32*, 4643–4655. (c) Grineva, A. A.; Filippov, O. A.; Canac, Y.; Sortais, J.-B.; Nefedov, S. E.; Lukan, N.; César, V.; Valyaev, D. A. Experimental and theoretical insights into the electronic properties of anionic N-heterocyclic dicarbenes through the rational synthesis of their transition metal complexes. *Inorg. Chem.* **2021**, *60*, 4015–4025.
- (38) Green, M. L. H. A new approach to the formal classification of the covalent compounds of the elements. *J. Organomet. Chem.* **1995**, *500*, 127–148.
- (39) Chaquin, P.; Canac, Y.; Lepetit, C.; Zargarian, D.; Chauvin, R. Estimating local bonding/antibonding character of canonical molecular orbitals from their energy derivatives. The case of coordinating lone pair orbitals. *Int. J. Quantum Chem.* **2016**, *116*, 1285–1295.
- (40) (a) Bianchi, R.; Gervasio, G.; Marabello, D. Experimental Electron Density Analysis of Mn₂(CO)₁₀: Metal-Metal and Metal-Ligand Bond Characterization. *Inorg. Chem.* **2000**, *39*, 2360–2366. (b) Espinosa, E.; Alkorta, I.; Elguero, J.; Molins, E. From weak to strong interactions: a comprehensive analysis of the topological and energetic properties of the electron density distribution involving X-HF-Y systems. *J. Chem. Phys.* **2002**, *117*, 5529–5542.
- (41) Macchi, P.; Proserpio, D. M.; Sironi, A. Experimental Electron Density in a Transition Metal Dimer: Metal-Metal and Metal-Ligand Bonds. *J. Am. Chem. Soc.* **1998**, *120*, 13429–13435.
- (42) (a) Espinosa, E.; Molins, E.; Lecomte C. Hydrogen bond strengths revealed by topological analyses of experimentally observed electron densities. *Chem. Phys. Lett.* **1998**, *285*, 170–173. (b) Espinosa, E.; Alkorta, I.; Rozas, I.; Elguero, J.; Molins, E. About the evaluation of the local kinetic, potential and total energy densities in closed-shell interactions. *Chem. Phys. Lett.* **2001**, *336*, 457–461.
- (43) Petitjean, H.; Lepetit, C.; Nour, Z.; Poteau, R.; del Rosal, I.; Berthomieu, D. How Cu^I and Na^I interact with Faujasite Zeolite? A theoretical investigation. *J. Phys. Chem. C* **2020**, *124*, 28026–28037.

- (44) (a) Poyatos, M.; Maise-François, A.; Bellemin-Laponnaz, S.; Gade, L. H. Coordination chemistry of a modular N,C-chelating oxazole-carbene ligand and its applications in hydrosilylation catalysis. *Organometallics* **2006**, *25*, 2634–2641. (b) Vuong, K. Q.; Timerbulatova, M. G.; Peterson, M. B.; Bhadbhadea, M.; Messerle, B. A. Cationic Rh and Ir complexes containing bidentate imidazolylidene–1,2,3-triazole donor ligands: synthesis and preliminary catalytic studies. *Dalton Trans.* **2013**, *42*, 14298–14308.
- (45) Palatinus, L.; Chapuis, G. Superflip – a computer program for the solution of crystal structures by charge flipping in arbitrary dimensions. *J. Appl. Cryst.* **2007**, *40*, 786–790.
- (46) Betteridge, P. W.; Carruthers, J. R.; Cooper, R. I.; Prout, K.; Watkin, D. J. Crystals version 12: software for guided crystal structure analysis. *J. Appl. Cryst.* **2003**, *36*, 1487.
- (47) Blessing, R. H. An empirical correction for absorption anisotropy. *Acta Crystallogr.* **1995**, *A51*, 33–38.
- (48) van der Sluis, P.; Spek, A. L. BYPASS: an effective method for the refinement of crystal structures containing disordered solvent regions. *Acta Cryst.* **1990**, *A46*, 194–201.
- (49) Frisch, M. J.; Trucks, G. W.; Schlegel, H. B.; Scuseria, G. E.; Rob, M. A.; Cheeseman, J. R.; Jr, J.A.M.; Vreven, T.; Kudin, K. N.; Burant, J. C.; Millam, J. M.; Iyengar, S. S.; Tomasi, J.; Barone, V.; Mennucci, B.; Cossi, M.; Scalmani, G.; Rega, N.; Petersson, G. A.; Nakatsuji, H.; Hada, M.; Ehara, M.; Toyota, K.; Fukuda, R.; Hasegawa, J.; Ishida, M.; Nakajima, T.; Honda, Y.; Kitao, O.; Nakai, H.; Klene, M.; Li, X.; Knox, J. E.; Hratchian, H. P.; Cross, J. B.; Bakken, V.; Adamo, C.; Jaramillo, J.; Gomperts, R.; Stratmann, R. E.; Yazyev, O.; Austin, A. J.; Cammi, R.; Pomelli, C.; Ochterski, J. W.; Ayala, P. Y.; Morokuma, K.; Voth, G. A.; Salvador, P.; Dannenberg, J. J.; Zakrzewski, V. G.; Dapprich, S.; Daniels, A. D.; Strain, M. C.; Farkas, O.; Malick, D. K.; Rabuck, A. D.; Raghavachari, K.; Foresman, J. B.; Ortiz, J. V.; Cui, Q.; Baboul, A. G.; Clifford, S.; Cioslowski, J.; Stefanov, B. B.; Liu, G.; Liashenko, A.; Piskorz, P.; Komaromi, I.; Martin, R. L.; Fox, D. J.; Keith, T.; Al-Laham, M. A.; Peng, C. Y.; Nanayakkara, A.; Challacombe, M.; Gill, P. M. W.; Johnson, B.; Chen, W.; Wong, M. W.; Gonzalez, C.; Pople, J. A. *Gaussian 09, Revision D.01*, Gaussian, Inc., Wallingford, CT, 2009.
- (50) Ehlers, A.W.; Böhme, M.; Dapprich, S.; Gobbi, A.; Höllwarth, A.; Jonas, V.; Köhler, K. F.; Stegmann, R.; Veldkamp, A.; Frenking, G. A set of f-polarization functions for pseudo-potential basis sets of the transition metals Sc–Cu, Y–Ag and La–Au. *Chem. Phys. Lett.* **1993**, *208*, 111–114.
- (51) Keith, T. A. AIMAll (Version 17.11.04), TK Gristmill Software, Overland Park KS, USA, aim.tkgristmill.com.
- (52) Bader, R. F. W. in *Atoms In Molecules*; Clarendon Press: Oxford, UK. **1990**.

Table of Contents artwork and text



Phosponium ylide core C,C,C -Pd(II) pincer complexes, cationic or zwitterionic in nature depending on the ylide *trans*-coordinated ligand, are readily prepared from *N*-phosponio-substituted imidazolium salt.
